Dinocyst stratigraphy of the Valanginian–Aptian Rurikfjellet and Helvetiafjellet formations on Spitsbergen, Arctic Norway

Journal:	*Geological Magazine*
Manuscript ID	GEO-19-2278.R1
Manuscript Type:	Original Article
Date Submitted by the Author:	04-Sep-2019
Complete List of Authors:	Śliwińska, Kasia; Geological Survey of Denmark and Greenland, Stratigraphic Department Jelby, Mads; University of Copenhagen, Department of Geosciences and Natural Resource Management Grundvåg, Sten-Andreas; UiT Arctic University of Norway, Department of Geosciences Nøhr-Hansen, Henrik; Geological Survey of Denmark and Greenland, Stratigraphy Alsen, Peter; Geological Survey of Denmark and Greenland, Stratigraphic Department Olaussen, Snorre; University Centre in Svalbard
Keywords:	dinocysts, biostratigraphy, Lower Cretaceous, Spitsbergen, Arctic

Dinocyst stratigraphy of the Valanginian–Aptian Rurikfjellet and Helvetiafjellet formations on Spitsbergen, Arctic Norway

Kasia K. Śliwińska(1), Mads E. Jelby(2), Sten-Andreas Grundvåg(3), Henrik Nøhr-Hansen(1), Peter Alsen (1), Snorre Olaussen(4)

(1) Department of Stratigraphy, Geological Survey of Denmark and Greenland (GEUS), Øster Voldgade 10, DK-1350 Copenhagen K, Denmark (kksl@geus.dk, hnh@geus.dk)

(2) Department of Geosciences and Natural Resource Management, University of Copenhagen, Øster Voldgade 10, DK-1350 Copenhagen K, Denmark (madsjelby@gmail.com)

(3) Department of Geosciences, UiT The Arctic University of Norway, P.O. Box 6050, Langnes, N-9037 Tromsø, Norway (Sten-Andreas.Grundvag@uit.no)

(4) Department of Arctic Geology, The University Centre in Svalbard (UNIS), P.O. Box 156, N-9171 Longyearbyen, Norway (Snorre.Olaussen@unis.no)

Abstract

In order to improve the understanding of how the high northern latitudes responded to the escalating warming which led to the middle Cretaceous super greenhouse climate, more temperature proxy records from the High Arctic are needed. One of the current obstacles in obtaining such records is poor age control on the Lower Cretaceous strata in the Boreal and Pan-Boreal regions.

Here, we provide a biostratigraphic framework for the Rurikfjellet and Helvetiafjellet formations representing the lower part of the Lower Cretaceous succession on Spitsbergen. We also attempt to date the boundary between the Agardhfjellet and the Rurikfjellet formations. This study is based on dinoflagellate cysts (dinocysts) from three onshore cores (DH1, DH2, and DH5R), and three outcrop sections (Bohemanflya, Myklegardfjellet, and Ullaberget). Relatively abundant and well-preserved dinocyst assemblages from the Rurikfjellet Formation date this unit as early Valanginian – early Barremian. The dinocyst assemblages from the Helvetiafjellet Formation are significantly impoverished and are characterised by reworking, but collectively indicate a Barremian–Aptian age for this formation.

Keywords: dinocysts, biostratigraphy, Lower Cretaceous, Spitsbergen, Arctic

1. Introduction

The Early Cretaceous (~145–100.5 Ma; Ogg, Ogg & Gradstein, 2016) was characterised by major tectonic activity, climatic changes, and global perturbations in

the carbon cycle (e.g. Huber *et al.*, 2018). The breakup of the supercontinent Pangaea which terminated around 175 Ma (e.g. Holden, 1970; Rogers & Santosh, 2004), led to the formation of two minor supercontinents: Laurasia to the north, and Gondwana to the south separated by the newly formed Tethys Ocean. The Barents Sea Shelf including Svalbard (paleolatitude 60°N at 140 Ma; calculated after Van Hinsbergen *et al.*, 2015), Arctic Canada, Greenland and northern Russia were located at the northern flank of Laurasia as part of the large circum-Arctic, relatively cold Boreal Basin (Scotese, 2014). In the Tethys Ocean to the south, warm to tropical water conditions prevailed, leading to a bloom of calcareous nannoplankton and foraminifera. The Tethys and Boreal seas were connected by a shallow, narrow seaway between Greenland and Baltica. The seaway formed in response to rifting during the initial stage of the formation of the North Atlantic Ocean at that time (e.g. Gradstein, Kaminski & Agterberg, 1999). The palaeogeographical configuration in the Early Cretaceous favoured a diversification of marine organisms and diachroniety of ammonite bio-events, which traditionally constitute the primary tool for Cretaceous biostratigraphy (e.g. Lehmann, 2015). This has led to the creation of two separate biozonation schemes; one for the Boreal and one for the Tethyan Realm. Both are still applicable across the Jurassic–Cretaceous transition (Ogg, Hinnov & Huang, 2012).

Temperature proxy data from Early Cretaceous high latitudes are limited (Ditchfield, 1997; Littler *et al.*, 2011; Jenkyns *et al.*, 2012; Price and Passey, 2013), but it is assumed that the global climate was generally warm and humid with low latitudinal temperature gradients (e.g. O'Brien *et al.*, 2017). In contrast, some studies suggest that the polar regions during the Early Cretaceous were rather cold (e.g. De Lurio and

Frakes, 1999; Basov *et al.*, 2009). Increased volcanic activity (including oceanic crust formation, formation of large igneous provinces, and subduction-related arc volcanism) (e.g. Johnston, Turchyn & Edmonds, 2011; Koopmann *et al.*, 2014; Polteau *et al.*, 2016) forced an increased concentration of atmospheric greenhouse gases (methane and CO_2), and led to a gradual global warming (e.g. Huber *et al.*, 2018). A climatic maximum of this extreme global warmth, the so-called Cretaceous Hot Greenhouse climate, was reached between 95 and 80 Ma (Huber *et al.*, 2018). During the Cretaceous Period a number of oceanic anoxic events (OAEs) led to the deposition of organic carbon-rich sediments (Leckie, Bralower & Cashman, 2002; Trabucho Alexandre *et al.*, 2010). At least four of these events took place during the Early Cretaceous: The OAE1a, OAE1b, OAE1c, and OAE1d (Erbacher, Thurow and Littke, 1996). The most widely recognised is the OAE1a which occurred during the earliest Aptian (Leckie, Bralower and Cashman, 2002; Jenkyns, 2010; Herrle *et al.*, 2015; Midtkandal *et al.*, 2016). The characteristic stable carbon isotope ($\delta^{13}C$) excursions related to OAEs can be used for the correlation of carbon isotope records (Herrle *et al.*, 2015; Midtkandal *et al.*, 2016; Vickers *et al.*, 2016). However, while the climatic history of the Tethys (e.g. Hochuli *et al.*, 1999; Bottini *et al.*, 2015; Bottini and Erba, 2018) and the European Boreal Realm (e.g. Mutterlose, Pauly & Steuber, 2009) are relatively well-studied, the climate of the Early Cretaceous Arctic is relatively less understood. Many of the published paleotemperature records contradict evidence for both warm and cool periods (e.g. Galloway *et al.*, 2015; Hurum, Druckenmiller, *et al.*, 2016; discussion in Vickers *et al.*, 2016). Some of the contradictions may be due to limited temperature data from the high

Arctic and the lack of a concise biostratigraphic framework for the Cretaceous strata in this region.

On Spitsbergen (Svalbard, Arctic Norway) the Lower Cretaceous succession is divided into three formations: the Rurikfjellet, Helvetiafjellet and Carolinefjellet formations. The first biostratigraphic study of the Rurikfjellet Formation was based on macrofossils (bivalves and ammonites), and dated the formation as Berriasian – upper Hauterivian (for references see Grøsfjeld 1991). The first dinocyst-based study of the Lower Cretaceous succession on Spitsbergen was provided by Bjærke and Thusu (1976). The first comprehensive study of Lower Cretaceous dinocysts on Spitsbergen was carried out by Bjærke (1978), who observed that the dinocyst assemblages of the Berriasian, Valanginian and Hauterivian are similar to assemblages from NW Europe and Arctic Canada.

The aim of this paper is to provide a concise age model for the Lower Cretaceous Rurikfjellet and Helvetiafjellet formations on Spitsbergen. The study is primarily based on dinocysts from six onshore outcrop and sediment core sections. The new data are discussed in the context of existing literature dealing with the palynology of the Arctic and the European Boreal Province.

2. Regional setting

Spitsbergen is the largest island in the Svalbard archipelago, and is located today at ca. 76–80°N. The Svalbard archipelago represents the uplifted and exposed northwestern corner of the Barents Sea Shelf. The Barents Sea Shelf is bounded to the west by the

Western Barents Sea Margin, and to the south and east by the Baltic Shield and Novaya Zemlya archipelago (e.g. Henriksen *et al.*, 2011). During the Early Cretaceous, the Svalbard platform was part of a shallow, epicontinental sag basin (e.g. Henriksen *et al.*, 2011) on the northern margin of Pangea (Torsvik *et al.*, 2002). The Lower Cretaceous succession in Svalbard is over 1000 m thick and exhibits a large-scale regressive–transgressive stacking pattern. This depositional cycle was controlled by regional thermo-tectonic uplift in the north, followed by subsequent quiescence and subsidence (Gjelberg & Steel, 1995; Midtkandal, Nystuen & Nagy, 2007; Midtkandal & Nystuen, 2009). The magmatic activity in Svalbard and the surrounding areas related to the emplacement of the High Arctic Large Igneous Province (HALIP) peaked in the Barremian to early Aptian (Corfu *et al.*, 2013; Senger *et al.*, 2014; Polteau *et al.*, 2016). An early Barremian uplift and associated southward tilting of the shelf caused the formation of a regionally extensive subaerial unconformity, which now forms the boundary between the Rurikfjellet and Helvetiafjellet formations (e.g. Gjelberg & Steel, 1995; Midtkandal & Nystuen, 2009; Grundvåg *et al.*, 2017). This event was followed by a transgression related to a long-term relative global sea-level rise (Gjelberg and Steel, 1995; Midtkandal and Nystuen, 2009). In the Late Cretaceous, subaerial exposure of Svalbard resulted in a major hiatus spanning the entire Upper Cretaceous (Harland, 1997; Dörr *et al.*, 2012).

<<Fig. 1>>

3. Lower Cretaceous lithostratigraphy of Spitsbergen

The Lower Cretaceous succession on Spitsbergen is subdivided into the Rurikfjellet, Helvetiafjellet and Carolinefjellet formations. The succession forms the upper part of the Adventdalen Group (which also includes the Upper Jurassic Agardhfjellet Formation; Parker, 1967), and is primarily exposed along the margins of the Central Tertiary Basin. The Rurikfjellet Formation consists of a lower offshore shale-dominated succession (the Wimanfjellet Member) which is overlain by a storm-dominated shallow marine succession (the Kikutodden Member) of interbedded shale, siltstone, and sandstone (Fig.1). The Rurikfjellet Formation unconformably overlies the Upper Jurassic – lowermost Cretaceous Agardhfjellet Formation (Dypvik *et al.*, 1991), and its base is marked either by i) a condensed glauconitic clay unit (the Myklegardfjellet Bed; Dypvik *et al.*, 1991; Dypvik, Nagy & Krinsley, 1992); ii) a highly tectonised decollement zone; or iii) by an abrupt change in the macrofossil fauna. In the central part of Spitsbergen, the Wimanfjellet Member is intersected by a thick succession of gravity flow deposits informally defined as the Adventpynten member (Grundvåg *et al.*, 2017). The Kikutodden Member represents prodeltaic to shallow marine deposits which were sourced from the NW and exhibit progradation towards the SE (Fig. 1; Dypvik *et al.*, 1991). The overall changes in the lithologies of the Rurikfjellet Formation reflect the shallowing development of the basin as a response to uplift in the north.

The boundary between the Rurikfjellet and Helvetiafjellet formations is marked by a regionally extensive subaerial unconformity (e.g. Midtkandal & Nystuen, 2009; Grundvåg *et al.*, 2017). The Helvetiafjellet Formation represents a fluvio-deltaic to paralic depositional system reflecting long-term relative sea-level rise (Gjelberg and Steel, 1995; Midtkandal and Nystuen, 2009). The Helvetiafjellet Formation represents

the most proximally deposited strata within the Lower Cretaceous succession on Spitsbergen. The Helvetiafjellet Formation is overlain by storm-dominated open marine shelf deposits of the Carolinefjellet Formation (Gjelberg and Steel, 1995; Grundvåg *et al.*, 2017); Fig. 1.

4. Previous studies of Lower Cretaceous Boreal dinocyst assemblages

Dinocyst studies of Arctic Lower Cretaceous successions are relatively rare and scattered across the Canadian Arctic (Pocock, 1976; Brideaux, 1977; McIntyre & Brideaux, 1980; Davies, 1983; Nøhr-Hansen & McIntyre, 1998), Greenland (Nøhr-Hansen, 1993; Pedersen & Nøhr-Hansen, 2014; Piasecki, Nøhr-Hansen & Dalhoff, 2018; Nøhr-Hansen, Piasecki & Alsen, this issue), the Barents Sea (Århus *et al.*, 1990; Smelror *et al.*, 1998; Smelror and Dypvik, 2005b, 2005a; Kairanov *et al.*, 2018), Arctic Norway (Løfaldi and Thusu, 1976; Thusu, 1978; Bjærke, 1978; Århus, Verdenius and Birkelund, 1986; Århus *et al.*, 1990; Århus, 1991; Grøsfjeld, 1991; Smelror and Larssen, 2016; Hurum, Roberts, *et al.*, 2016; Smelror *et al.*, 2018; Hammer *et al.*, 2018; Rakociński *et al.*, 2018; Grundvåg *et al.*, 2019), and Arctic Russia (Smelror, 1986; Lebedeva and Nikitenko, 1999; Riding, 1999; Pestchevitskaya, 2007; Nikitenko *et al.*, 2008; Pestchevitskaya, Lebedeva and Ryabokon, 2011). Some early Canadian studies provided dinocyst zonations (e.g. Pocock, 1976; Davey, 1982; Davies, 1983), but the diversity of the studied material was limited, and ranges of specific taxa were poorly constrained compared to the more recent and robust dinocyst zonation established for North-East Greenland (Nøhr-Hansen, 1993; Nøhr-Hansen, Piasecki & Alsen, this issue). A number of dinocyst studies from the North Sea Basin and

northwest Europe, often referred to as the European Boreal Province, provide well-constrained zonation schemes (Davey, 1979a, 1982; Heilmann-Clausen, 1987; Costa & Davey, 1992; Duxbury, 2001; Bailey, 2019).

The first chronostratigraphic framework for the Rurikfjellet Formation (at that time known as the Rurikfjellet Member) was based on ammonites and bivalves (for references see Grøsfjeld, 1991). An informally defined Lower Cretaceous palynological zonation of Spitsbergen was introduced in a confidential report by Århus (1988). Low dinocyst abundances and low diversities have been reported from studies of the Lower Cretaceous succession on Spitsbergen and in the Barents Sea (e.g. Århus *et al.*, 1990; Århus, 1992). The dinocysts of the Rurikfjellet Formation have been investigated in less than a dozen peer-reviewed publications. Notable works include Bjærke & Thusu (1974), Bjærke (1978), Århus *et al.* (1990), Århus (1991; 1992), Grøsfjeld (1991), and more recently Midtkandal *et al.* (2016) and Grundvåg *et al.* (2017). The palynology of the Helvetiafjellet Formation has been studied to an even lesser extent (Grøsfjeld, 1991; Midtkandal *et al.*, 2016). A number of recent studies on the seismic stratigraphy of the Lower Cretaceous succession in the southwestern Barents Sea provide an updated preliminary age model based on dinocysts (Marin *et al.*, 2017; Kairanov *et al.*, 2018; Marín, Escalona, Grundvåg, Nøhr-Hansen, *et al.*, 2018; Marín, Escalona, Grundvåg, Olaussen, *et al.*, 2018).

5. Studied sections

5.a. The Bohemanflya outcrop section

The Bohemanflya outcrop section (N78°24'32.6"/E14°41'18.9") is the northernmost locality investigated in this study, exposing Lower Cretaceous strata in central Spitsbergen (Fig. 2). At this locality, the Wimanfjellet Member constitutes a measurable thickness of c. 45 m and consists of generally black shale with scattered siderite concretions and nodules or stratabound siderite layers. In certain intervals, the Wimanfjellet Member is tectonically disturbed. The overlying Kikutodden Member (Fig. 1) is c. 83 m thick, and is siltstone- and sandstone-dominated. The upper part of the succession exhibits gravel-rich hummocky cross-stratified sandstone, which is occasionally truncated by the subaerial unconformity constituting the base of the overlying Festningen Member of the Helvetiafjellet Formation. In this study, we collected samples from across the entire exposed length of the Rurikfjellet Formation (~130 m; Fig. S1).

<<Fig.2>>

5.b. The Myklegardfjellet outcrop section

The Myklegardfjellet outcrop section (N78°03'18.8"/E18°42'15.4") is the easternmost locality investigated in this study, exposing Upper Jurassic – Lower Cretaceous strata at the northeastern side of Agardhbukta, east coast of Spitsbergen (Fig. 2). At this locality, the Rurikfjellet Formation is entirely comprised of homogeneous shale of the Wimanfjellet Member (Fig. 1), reaching a thickness of 166 m. The shale is characterised by absent to low degrees of bioturbation as well as scattered siderite concretions, nodules and fossiliferous stratabound siderite layers with abundant bivalves. The Kikutodden Member is either not preserved in this locality, or it is covered by scree. This outcrop section is the type locality of the Myklegardfjellet Bed (Birkenmajer,

Pugaczewska & Wierzbowski, 1979; Dypvik, Nagy & Krinsley, 1992), demarcating the base of the Rurikfjellet Formation by a well-exposed c. 3 m thick unit of glauconitic, plastic clays. The Rurikfjellet Formation is unconformably overlain by sandstones of the Festningen Member of the overlying Helvetiafjellet Formation. In this study we investigate ca. 130 m of deposits from the Wimanfjellet Member (Fig. S2).

5.c. The Ullaberget outcrop section

The Ullaberget outcrop section (N77°37'04.2"/E15°11'17.9") is the southernmost locality investigated in this study, exposing Lower Cretaceous strata at the northwestern side of Van Keulenfjorden. At this locality, the Rurikfjellet Formation is ca. 200 m thick (the base is not exposed) and dominated by homogeneous shale of the Wimanfjellet Member. For the purpose of this study, only three samples from the uppermost 2 metres of the Rurikfjellet Formation were collected (Fig. S3). The shale is characterised by a lack of or low degrees of bioturbation. Siderite concretions, nodules, and fossiliferous stratabound layers occur. Thin- and lenticular-bedded sandstone occurs sporadically in the upper part of the unit, representing the distal part of the Kikutodden Member. The Rurikfjellet Formation is unconformably overlain by sandstones of the Louiseberget Bed of the Helvetiafjellet Formation (Midtkanal *et al.*, 2008). The remaining part of the Helvetiafjellet Formation displays a transgressive development, comprising various paralic deposits, including tidal channel fills, and coarsening-upwards bay fill sequences (Gjelberg & Steel, 1995; Midtkandal & Nystuen, 2009) which lithostratigraphically belong to the Glitrefjellet Member. At this locality, the Helvetiafjellet Formation is conformably overlain by a 20–30 m thick shale unit of the Carolinefjellet Formation.

5.d. The DH1 and DH2 cores

The DH1 (N78°23'60.8/E15°54'57.6) and DH2 (N78°23'59.9/E15°54'68.4) cores were drilled c. 3 km to the NW of Longyearbyen close to the airport, in relation to CO_2 sequestration studies (Braathen *et al.*, 2012). The cores span the Rurikfjellet and Helvetiafjellet formations, and the lower part of the Carolinefjellet Formation (Fig. 1). In these wells, the Rurikfjellet Formation is ca. 225 m thick (~440–215 m) and conformably overlies shale of the Agardhfjellet Formation (e.g. Grundvåg *et al.*, 2017). The boundary between the two units is tectonically disturbed, representing a decollement zone that formed during the Palaeogene shortening (Dietmar Müller & Spielhagen, 1990). The lower part of the Rurikfjellet Formation consists of a ~140 m thick succession of gravity flow deposits of the Adventpynten member. The upper part of the Rurikfjellet Formation consists of a 30–40 m thick mudstone-dominated unit which grades upwards into the sandstone-dominated Kikutodden Member. The Rurikfjellet Formation is unconformably overlain by a 12 m thick sandstone unit representing the Festningen Member of the Helvetiafjellet Formation (Grundvåg *et al.*, 2017). The upper c. 60 m of the Helvetiafjellet Formation consists of interbedded sandstone, shale, and thin coal layers of the Glitrefjellet Member, representing various alluvial to paralic depositional environments. The thicknesses of all lithostratigraphic units across the investigated interval in the two cores are shown on Fig. S4 (DH1) and Fig. S5 (DH2). The Helvetiafjellet Formation is unconformably overlain by a ~10 m thick shale unit of the overlying Dalkjegla Member of the Carolinefjellet Formation.

5.e. The DH5R core

The DH5R core (N78°12'13.1"/E15°49'08.6") was drilled c. 4 km to the SE of Longyearbyen in central Spitsbergen, also in relation to CO_2 sequestration studies (Braathen *et al.*, 2012). The studied part of the core spans from the uppermost Agardhfjellet Formation to the Carolinefjellet Formation. The Rurikfjellet Formation is c. 230 m thick (410–180 m) and overlies shale of the Agardhfjellet Formation (Koevoets *et al.*, 2018). The lithology of the Rurikfjellet Formation differs from that observed in the DH1 and DH2 cores. In the DH5R core, the formation displays homogeneous to sparsely bioturbated shale with scattered siderite concretions and bivalves of the Wimanfjellet Member which coarsen into silty shale, heavily bioturbated siltstone and hummocky cross-stratified sandstone of the overlying Kikutodden Member. The Helvetiafjellet (180–120 m) and Carolinefjellet formations display the same stratigraphic development as in the DH1, and DH2 cores.

6. Analytical methods

Sediment samples for palynological analysis were collected during fieldwork and core logging campaigns in 2013–2016. 82 samples were collected, with 40 samples from Bohemanflya, Myklegardfjellet and Ullaberget, and 42 samples from the DH1, DH2, and DH5R cores. The majority of samples were collected from the Rurikfjellet Formation, including 8 samples from DH1, 14 samples from DH2, 15 samples from DH5R, 12 samples from Bohemanflya, 13 samples from Myklegardfjellet and 3 samples from Ullaberget. The Helvetiafjellet Formation was sampled only in the DH2 core (3 samples) and Ullaberget outcrop section (12 samples). Furthermore, in order to improve the age

of the base of the Lower Cretaceous succession in our study area, we have analysed three samples from the upper part of the Agardhfjellet Formation from the DH5R core (at 458.0, 440.0, and 410.0 m).

Preparation of palynological slides was performed at the Geological Survey of Denmark and Greenland (GEUS). Between 20 and 45 g of sediment were dried in an oven for 24 hours at 30ºC and manually ground. Hydrochloric (HCl; 3.5% and 18%) and hydrofluoric (HF; 40%) acids were used for dissolving carbonates and silicates, respectively. After each step, samples were neutralized with 0.5% citric acid ($C_6H_8O_7$) at 70°C. The organic residuum from each sample was filtered using an 11 µm nylon mesh and a first (kerogen) slide was prepared. Subsequently, the residua were oxidized with HNO_3 for 8 min in order to remove amorphous kerogen particles. Samples with high concentrations of amorphous kerogen particles were oxidized for additional 1 to 5 min. After each oxidation step, residua were washed with a weak solution (5%) of potassium hydroxide (KOH), and a fraction of the residue was taken for palynological slide preparation. Some of the residua were additionally briefly submerged in a boiling mixture of HNO_3:KOH (1:1), and filtered using a 21 µm nylon mesh. The high concentration of coal and wood particles present in some of the samples was removed by swirling, and minerals were removed by heavy liquid separation (ZnBr; density 2.3 g/mL). After each of these steps, organic residua were filtered using a 21 µm nylon mesh. To concentrate palynomorphs, organic residua from some of the samples were filtered using a 30 µm nylon mesh. All palynological slides and (if available) organic residua are stored at GEUS.

The palynological slides were analysed using a transmitted light microscope. When possible, a minimum of 300 dinocysts were counted in a single slide. In a few cases, when a single slide contained less than 300 dinocysts, it was necessary to count one or two additional slides. The dinocyst taxonomy follows Williams, Fensome & MacRae (2017). All dinocysts recorded in this study are listed in Table 1. Selected dinocysts are presented on Figs. 3-6. Coordinates of the photographed specimens are given following the method described by Śliwińska (2019).

<<Fig.3>>

<<Fig. 4>>

<<Fig.5>>

<<Fig. 6>>

7. Results and discussion

Two out of three samples from the Agardhfjellet Formation were barren with respect to dinocysts. Virtually all analysed samples from the Rurikfjellet Formation and the Helvetiafjellet Formation yielded dinocysts. The diversity, abundance and preservation are highly variable spatially and temporally. In samples where dinocysts were rare or absent, the assemblages are dominated by black and dark brown wood particles, as well as pollen grains.

In some levels, despite counting more than one palynological slide, there were less than 300 dinocysts in total (e.g. in the uppermost samples of the DH5R core). The dinocyst assemblages were particularly impoverished in the Ullaberget outcrop section,

and in the DH1 and DH2 cores. In comparison, the dinocyst assemblages of the Myklegardfjellet outcrop section show the highest richness of species (Fig. S2).

Within the Rurikfjellet Formation we distinguish several age-diagnostic dinocysts: *Endoscrinium hauterivianum* (Figs 3o,p; Section 8.a), *Gochteodinia villosa* subsp. *villosa* (Fig. 4b; Section 8.b), *Muderongia australis* (Fig. 4e; Section 8.c), *Muderongia tetracanta* (Fig. 4d; Section 8.d), *Nelchinopsis kostromiensis* (Figs 4m,n; Section 8.e), *Oligosphaeridium complex* (Fig. 5h; Section 8.f), *Palaecysta palmula* (Fig. 5k; Section 8.i), *Subtilisphaera perlucida* (Fig. 6g; Section 8.l), and *Tubotuberella apatela* (Figs 6i-k; Section 8.m). Other typical dinocysts observed within the formation include *Cyclonephelium cuculliforme* sensu Århus 1990 (Fig. 5l), *Discorsia nannus* (Fig. 3m), *Dissiliodinium acmeum* (Figs 3k), *Nyktericysta? pannosa* (Figs 4op), *Oligosphaeridium abaculum* (Fig. 5f; Section 8.g), *Phoberocysta neocomica* (Fig. 5c), *Pseudoceratium pelliferum* (Fig. 5j), *Rhynchodiniopsis aptiana* (Fig. 5d,g), *Stanfordella fastigiata* (Fig 6a), *Stanfordella ordocava* (Figs 6b,c), and *Wrevittia perforobtusa* (Figs 6n-p). Notably, some of the well-known Lower Cretaceous markers, such as e.g. *Batioladinium longicornutum*, were not observed in the studied material.

The age-diagnostic taxa within the Helvetiafjellet Formation include *Odontochitina nuda* (Fig. 5e; Section 8.f), *Pseudoceratium anaphrissum* (Figs 5m-o; Section 8.j), *Sirmiodinium grossii* (Figs 6e,f; Section 8.k), and *Subtilisphaera perlucida* (Fig. 6g; Section 8.l). The Helvetiafjellet Formation is also characterised by low species richness, low relative abundance of dinocysts and a moderate reworking of Valanginian to Barremian dinocysts.

The age of the first (FOs) and last occurrences (LOs) as well as ranges of the key dinocysts in the context of existing literature are discussed in Section 8.

<<Fig. 7>>

7.a. Palynological framework for the Agardhfjellet Formation

The two lowermost samples from the DH5R core collected from the upper part of the Agardhfjellet Formation (at 458.0 and 440.0 m) are barren of dinocysts (Figure S6). The sample at 410 m yields only few, poorly preserved dinocysts (Figure S6). In this sample, the co-occurrence of *Sirmiodinium grossii* and *Tubotuberella apatela* suggests a very broad Bathonian – early Valanginian age (e.g. Costa and Davey, 1992). Our dinocyst-derived age constrain is therefore not as good as the age based e.g. on macrofossils, which dates this part of the Agardhfjellet Formation as Ryazanian (Wierzbowski *et al.*, 2011).

7.b. Palynological framework for the Rurikfjellet Formation

The distribution of dinocysts in the Rurikfjellet Formation (except the Myklegardfjellet Bed; Fig. 1) from the studied sites suggests that this formation is of early Valanginian to possibly earliest Barremian age (Fig. 8).

The dinocyst assemblages in the DH1 and DH2 cores are characterised by poor preservation, low diversity and low dinocyst abundance. Both cores penetrate the ca.150 m thick gravity flow deposits of the Adventpynten member (Grundvåg *et al.*, 2017) that yield a number of reworked taxa. In the DH2 core, the lowermost samples from the Rurikfjellet Formation yield only a single highly corroded *Oligosphaeridium*

specimen (possibly *O. complex* or *O. asterigerum*). Thus, this interval is tentatively dated as Valanginian or younger (Fig. S5). The two lowermost samples from the DH1 well (corresponding to the base of the Rurikfjellet Formation according to Grundvåg *et al.*, 2017) also yield *O. complex* (Fig. S4). Furthermore, the sample at 414.0 m yields *Gochteodinia villosa* subsp. *multifurcata* while the sample at 410.2 m yields *Muderongia tetracantha* (Fig. S4). Thus, this interval is of Valanginian – Hauterivian age. The presence of *Endoscrinium hauterivianum* between 270.0 and 221.0 m implies that this interval is of early Hauterivian to earliest late Hauterivian age (see below). In summary, in the DH1 core (i.e. 414.0 to 221.0 m depth) the Rurikfjellet Formation is dated as Valanginian – earliest late Hauterivian (Fig. S4).

We find the best-constrained age for the basal part of the Rurikfjellet Formation (early Valanginian) to be represented by the Myklegardfjellet outcrop section (the interval from the base of the section up to level 60.0 m; Fig. S2). This notion is based on the co-occurrence of *Palaecysta palmula* and *O. complex* in the lowermost sample at 0.05 m. The early Valanginian age for the base of the Rurikfjellet Formation confirms previous observations (Bjærke, 1978; Århus, 1992).

The LO of the stratigraphically persistent *T. apatela* at 60.0 m in the Myklegardfjellet outcrop section is used here as a marker for the top of the early Valanginian, since most records agree that this bio-event is close to the early–late Valanginian boundary (see below; Fig. 7). This age assignment is in agreement with the presence of a *Tollia* (*Neocraspedites*) aff. *subtilis* ammonite of middle early Valanginian age found at 47.30 m (unpublished data of P. Alsen and M. E. Jelby).

In the DH5R core, the top of the stratigraphically persistent *Gochteodinia villosa* subsp. *villosa* is at 320.0 m, and it co-occurs with *O. complex* in the interval from 380.0 to 320.0 m. Based on these occurrences, we date this interval as earliest Valanginian. Placing the early–late Valanginian boundary close to the top of the persistent occurrence of these two taxa is in agreement with the observations by Århus (cf. Fig. 2 in Århus, 1992, and Enclosure 2 in Århus, 1988).

We place the base of the Hauterivian at the FO of *E. hauterivianum* (Fig. 8). The FO of *E. hauterivianum* is followed by the FO of *Muderongia tetracantha,* another important marker for the Hauterivian (e.g. Costa and Davey, 1992), Fig. 7. The stratigraphic range of *E. hauterivianum* observed in five sites (DH1, DH2, DH5R, Bohemanflya and Myklegardfjellet) in the middle to upper part of the Rurikfjellet Formation dates this part of the unit to the early Hauterivian – earliest late Hauterivian (Figs S4, S5, and 4). Grøsfjeld (1991) noted that *E. hauterivianum* (as *Apteodinium* sp. A of Bjærke,1978; Section 9.a.) is also present in several other outcrop sections of the Rurikfjellet Formation including Janusfjellet, Forkastningsfjellet and Helvetiafjellet.

Many samples from the uppermost part of the Rurikfjellet Formation in the DH1, DH2 and DH5R cores are characterised by low dinocyst abundance and relatively low species richness. The best age constrain for the top of the formation is therefore based on outcrop sections. The upper part of the Rurikfjellet Formation is dated to the late Hauterivian – earliest Barremian. The youngest part of the formation dated to the early Barremian is observed at Ullaberget and Bohemanflya.

In the Ullaberget outcrop section, two samples at 0.0 and 2.0 m, collected from the top of the Rurikfjellet Formation, yield *Pseudoceratium anaphrissum* and

Subtilisphaera perlucida. The sample at 0.0 m additionally yields *Nelchinopsis kostromiensis*, *P. anaphrissum*, and *S. perlucida*, which have their FOs close to the Hauterivian – Barremian boundary (Fig. S3). In the North Sea Basin, the LO of *N. kostromiensis* and the FO of *P. anaphrissum* are two important bio-events for recognition of the Hauterivian–Barremian boundary. Typically, the LO of *N. kostromiensis* marks the top of the Hauterivian, while the FO of *P. anaphrissum* marks the base of the Barremian (e.g. Costa & Davey, 1992). However, in some studies both bio-events are reported from the earliest Barremian (Heilmann-Clausen, 1987; Århus *et al.*, 1990; Smelror *et al.*, 1998; Bailey, 2019) or the uppermost Hauterivian (Nøhr-Hansen, 1993; Nøhr-Hansen, Piasecki & Alsen, this issue). In the North Sea, the ranges of these two species either overlap (Costa & Davey, 1992) or don't (Bailey, 2019). Overlapping ranges of the two taxa have been observed in North-East Greenland (Nøhr-Hansen, 1993; Nøhr-Hansen, Piasecki & Alsen, this issue). An overlap of the stratigraphic ranges of the two species was previously reported from the Barents Sea (well 7245/9-U-1) (Fig. 5 in Århus *et al.* 1990). Based primarily on the foraminifera assemblage, the overlap interval was dated as early Barremian (Århus *et al.*, 1990). However, these authors recognised that the presence of *Buchia sublaevis* bivalves within the same interval was problematic (p. 173 in Århus *et al.* 1990), because *Buchia* extends only into the Hauterivian (Zakharov, 1987). In summary, these observations give three possibilities for assigning an age to the LO of *N. kostromiensis* and the FO of *P. anaphrissum*: (i) In Spitsbergen, the Barents Sea and North-East Greenland, *P. anaphrissum* appears in latest Hauterivian; (ii) in Spitsbergen and the Barents Sea region, *N. kostromiensis* has a longer range reaching the earliest

Barremian; or (iii) *N. kostromiensis* occurring in the lower Barremian strata is reworked. We consider the first possibility to be the most plausible, since this is in agreement with other studies from the Arctic region (North-East Greenland, Barents Sea and Arctic Canada; cf. Fig. 7).

In the three uppermost samples from the Bohemanflya outcrop section (99.29 m to 132.63 m), we found a common to abundant dinocyst taxon previously recorded as *Nyktericysta*? *pannosa* by Grøsfjeld (1991). However, we observe that *N.*? *pannosa* from Bohemanflya (Figs 7o,p) with its generally less pronounced lateral horns differs from the holotype, which was described from "middle Barremian" strata from the Speeton Clay in England (Duxbury, 1980). Nevertheless, Grøsfjeld (1991), and this study show the only records of this taxon outside the type area. The restricted occurrence of *N.*? *pannosa* limited to the Bohemanflya section on Spitsbergen (Grøsfjeld 1991; this study) and to the Speeton Clay in England (Duxbury, 1980), could suggest that the distribution of the taxon is controlled by some environmental factors.

Based on the LO of *N. kostromensis* at 127.58 m and the presence of *N.*? *pannosa* between 99.29 m and 132.63 m, the interval is dated as latest Hauterivian – early Barremian.

In the topmost sample of the Myklegardfjellet outcrop section at 150.0 m, we observed an acme of *M. australis*. We consider this acme to be time-equivalent to the *M. australis* acme observed in the Barents Sea by Århus *et al.* (1990). Thus, we date this level as late Hauterivian – early Barremian.

Our new age framework for the Rurikfjellet Formation based on the dinocyst stratigraphy is in agreement with previous studies from the study area (e.g. Bjærke,

1978; Thusu, 1978; Århus, 1992; Midtkandal *et al.*, 2016), which dated the majority of the Rurikfjellet Formation as Valanginian – Hauterivian. Specifically, the Rurikfjellet Formation at the Janusfjellet outcrop section was previously dated as early Valanginian – late Hauterivian (Århus, 1992). We observe that our dinocyst distribution of the Myklegardfjellet outcrop section (Fig. S2) resembles the distribution of dinocysts from Janusfjellet (Enclosure 2 in Århus, 1988). Furthermore, our results confirm the observation by Grøsfjeld (1991) that the topmost part of the Rurikfjellet Formation is most likely of early Barremian age. Some reworking is present which is minor compared to the reworking in the Helvetiafjellet Formation (Figs. S1-S6).

<<Fig. 8>>

<<Fig.9>>

7.c. Palynological framework for the Helvetiafjellet Formation

We observe that the dinocyst assemblages of the Helvetiafjellet Formation are highly impoverished and yield a number of taxa reworked from the Rurikfjellet Formation. The reworking of Pliensbachian to Early Oxfordian dinoflagellate cysts within the Helvetiafjellet Formation was observed previously on Kong Karls Land (Smelror *et al.*, 2018). Redeposition is, however, not surprising, considering that the study area was uplifted and subaerially exposed in the Barremian with large parts of the Svalbard platform being subjected to erosion (Fig. 2).

Based on the presence of *Odontochitina nuda*, *Pseudoceratium anaphrissum*, *Sirmiodinium grossii* and *Subtilisphaera perlucida*, the Helvetiafjellet Formation is dated

here as Barremian to possibly early Aptian (Figs S3, S5 and 9). The boundary between the Rurikfjellet and Helvetiafjellet formations is dated as early Barremian. Due to the low diversity of the assemblages and rarity of dinocysts, it is not possible to precisely place the Barremian–Aptian boundary.

Our age assignment of the Helvetiafjellet Formation is in agreement with a recent stable carbon-isotope ($\delta^{13}C$) stratigraphic study of the Festningen outcrop section (Vickers *et al.*, 2016). These authors interpreted that the Helvetiafjellet Formation is of Barremian to earliest Aptian age. Another study, based on the U–Pb dating of a bentonite in the DH3 core (at 156.89 m in the middle part of the Helvetiafjellet Formation) suggested an age of 123.3 ± 0.2 Ma for this particular bed (Corfu *et al.*, 2013), corresponding to the late early Aptian (Ogg, Ogg & Gradstein, 2016) . However, the biostratigraphic framework of this study & Midtkandal *et al.* (2016) suggests that this part of the succession is of Barremian age. Nevertheless, the existing studies (e.g. Corfu *et al.*, 2013; Midtkandal *et al.*, 2016; Vickers *et al.*, 2016) collectively agree that the Helvetiafjellet Formation is of Barremian – early Aptian age.

8. Conclusions

The Rurikfjellet and Helvetiafjellet formations on Spitsbergen, Svalbard, have been studied in the DH1, DH2 and DH5R onshore cores as well as in the Bohemanflya, Myklegardfjellet and Ullaberget outcrop sections. Our study suggests an early Valanginian – early Barremian age for the Rurikfjellet Formation and a Barremian – Aptian age for the overlying Helvetiafjellet Formation. We provide a number of age diagnostic dinocyst bio-events for age determination of the Rurikfjellet and Helvetiafjellet

formations. The preservation of dinocysts is better and the diversity of assemblages is significantly higher in the offshore to shallow-marine Rurikfjellet Formation than in the fluvio-deltaic to paralic Helvetiafjellet Formation.

We observe some reworked dinocysts within the Helvetiafjellet Formation, possibly from the Rurikfjellet Formation. The presence of reworked dinocysts implies that any proxy records performed on bulk sediments (e.g. $\delta^{13}C$, biomarkers) across the Barremian – Aptian transition on Spitsbergen should be interpreted with care, since the signal may be biased.

We further observe that the distribution of *N.*? *pannosa* and *O. abaculum* is most likely controlled by local paleoenvironmental variations. For a better understanding of these records, further paleoenvironmental proxy data from the area are required.

The dinocyst assemblages in the three samples collected from the Agardhfjellet Formation are too impoverished to provide a reliable age constraint on the boundary between the Rurikfjellet and Argardhfjellet formations.

Our age model is in agreement with the existing stratigraphic studies carried out in the study area. Notably, our study provides the first comprehensive, semi-quantitative dataset of the distribution of dinocysts within the Lower Cretaceous (Valanginian–Aptian) succession on Spitsbergen.

9. Appendix A: Taxonomic notes on characteristic dinocyst taxa of the Rurikfjellet and Helvetiafjellet formations

9.a. Stratigraphic range of *Endoscrinium hauterivianum* (Duxbury, 2001) Riding & Fensome, 2003

Figs 3o,p

1978 *Apteodinium* sp. A (Bjærke, 1978)

1980? *Apteodinium* sp. A of Bjærke (1978) Bjærke plate X figs 1,2

1991 *Apteodinium* sp. A of Bjærke (1978) Grøsfjeld plate 4 figs D-F

2001 *Scriniodinium hauterivianum* Duxbury, 2001

2003 *Endoscrinium hauterivianum* (Duxbury, 2001) Riding & Fensome, 2003

The holotype of *E. hauterivianum* was described from the UK sector of the North Sea Basin (Duxbury, 2001). The taxon was described as restricted to the Hauterivian with the LO within the lowermost upper Hauterivian (Duxbury, 2001). We here suggest that *Apteodinium* sp. A of Bjærke (1978), which was recorded in the Valanginian to Hauterivian succession of the Rurikfjellet Formation (Bjærke, 1980), is a synonym of *E. hauterivianum*. Grøsfjeld (1991) noted that the species was present in numerous locations on Spitsbergen and can be used as a Hauterivian marker in the region. However, she also pointed out that at Janusfjellet the LO of *Apteodinium* sp. A of Bjærke (1978) postdates the LO of *N. kostromiensis* (for the stratigraphic range of *N. kostromiensis* see Section 9.e.) and thus it may range into the Barremian. Grøsfjeld (1991) did not observe *N. kostromiensis* in the Bohemanflya outcrop section (see Fig 6 in Grøsfjeld 1991), only *N*?. *pannosa* (see below) and *Apteodinium* sp. A of Bjærke (1978).

Spitsbergen - this study. In the present study *E. hauterivianum* is recorded in all studied sections. We apply the FO of *E. hauterivianum* as a marker for the base Hauterivian and the LO as the marker for the earliest late Hauterivian. In the two sections with the highest dinocyst diversity and the greatest abundance assemblage (Bohemanflya Fig. S1 and Myklegardfjellet, Fig. 5) the LO of *E. hauterivianum* predates the LO of *N. kostromiensis*. This is in contrast to the observations by Grøjsfjeld (1991) from the Bohemanflya outcrop section. We speculate that the longer range of *N. kostromensis* observed by us may be an effect of different sampling strategies carried in both studies. In the studied material the taxon is rare to abundant (i.e. <1% or >50% of the total dinocyst assemblage).

9.b. LO of *Gochteodinia villosa* (Vozzhennikova, 1967) Norris, 1978

Figs 4a-c

G. villosa is divided into two subspecies, *G. villosa* subsp. *villosa* (Vozzhennikova, 1967) and *G. villosa* subsp. *multifurcata* (Davey, 1982). The stratigraphic ranges of these subspecies are different (Fig. 7). The FO of *G. villosa multifurcata* postdates the FO of *G. villosa villosa* and thus distinguishing the two subspecies is very useful for increasing the resolution of the age framework. In the North Sea Basin *G. villosa multifurcata* ranges from the lower Valanginian (Heilmann-Clausen, 1987) to the lowermost Hauterivian (Heilmann-Clausen, 1987; Costa & Davey, 1992) or to the Valanginain–Hauterivian boundary (Davey, 1982; Bailey, 2019). The youngest LOs of

G. villosa villosa are reported at the Ryazanian–Valanginian boundary (Heilmann-Clausen, 1987) or in the earliest Valanginian (Costa and Davey, 1992; Bailey, 2019). Davey (1982) and Nøhr-Hansen, Piasecki & Alsen (this issue) reported the youngest occurrence of the taxon in the late Ryazanian–late Berriasian from Denmark and North-East Greenland, respectively. In the Sverdrup Basin, Arctic Canada, *G. villosa* (not differentiated into subspecies, and possibly *G. villosa multifurcata*) was found in the Valanginian (Davies, 1983). In the Barents Sea (possibly reworked) specimens of *G. villosa* were reported in the assemblages referred to the Hauterivian – lower Barremian (Århus *et al.*, 1990). Århus (1991) shows that on Central Spitsbergen *G. villosa* occurs in the Valanginian and Hauterivian strata, while *G. villosa multifurcata* has a slightly shorter range: Valanginian to lowermost Hauterivian. In the Valanginian part of the succession both taxa are present consistently. In post-Valanginian strata both taxa occur only sporadically (Fig. 13 in Århus, 1988) and thus their presence may be an effect of reworking.

Spitsbergen – this study. Specimens referred to *G. villosa villosa* and *G. villosa multifurcata* are slightly more elongate than the type material (cf. e.g. Davey, 1982). The poor preservation of some of the specimens encountered in the present study sometimes precludes an unambiguous separation of the two subspecies. We distinguish subspecies only if the determination is possible. In few samples *G. villosa* makes up 2–4 % of the total dinocysts assemblage. Otherwise, the species occurs persistently in the lower part of the Rurikfjellet Formation (Myklegardfjellet, DH5R), but is rather rare.

9.c. Stratigraphic range and abundance interval of *Muderongia australis* Helby, 1987

Fig. 4e

The youngest record on North-East Greenland of the taxon is from the upper Hauterivian (Nøhr-Hansen, 1993, Nøhr-Hansen, Piasecki & Alsen this issue). In the other few existing studies *M. australis* is reported either from the Hauterivian (Århus *et al.*, 1990; Prössl, 1990) or from the Barremian (Helby, 1987; Davey, 1988). In Spitsbergen *M. australis* is restricted to the upper part of the Rurikfjellet Formation (Århus *et al.*, 1990). Århus et al. (1990) also noted an acme of *M. australis* in the interval referred to the Hauterivian – early Barremian and mentioned that the *M. australis* acme may be related to the early Barremian flooding event.

Spitsbergen – this study. We observe the persistent occurrence of *M. australis* in the upper part of the Rurikfjellet Formation within all the studied sites. Thus, we confirm the observations of Århus et al. (1990). In the topmost sample from the Rurikfjellet Formation at the Myklegardfjellet outcrop *M. australis* occurs as a local acme, which we interpret to be synchronous with the acme observed in the Barents Sea (Århus et al. 1990) and North-East Greenland (Nøhr-Hansen, 1993).

8.d. *Muderongia extensiva* and *Muderongia tetracantha*

Figs 4d,g,h

In the North Sea Basin the LO of *M. extensiva* is a well established earliest Hauterivian marker (Heilmann-Clausen, 1987; Costa & Davey, 1992; Duxbury, 2001). *M.tetracantha* has a slightly younger range from the Hauterivian to the earliest Barremian (Costa and Davey, 1992; Duxbury, 2001) or even Aptian (Heilmann-Clausen, 1987; Nøhr-Hansen, 1993; Nøhr-Hansen and McIntyre, 1998). Notably, some authors merge *M. tetracantha* with *Muderongia crucis* (Costa and Davey, 1992; Bailey, 2019) or consider *M. crucis* as a junior synonym (e.g. Helby, 1987). Nevertheless, *M. tetracantha* is considered the most typical taxon for Hauterivian – lower Barremian strata (see discussion in Heilmann-Clausen, 1987). More details concerning the stratigraphic ranges of these two taxa in the Boreal and the European Boreal realm is shown on Fig. 7.

The morphologies of the two taxa are distinctive. The lateral horns of *M. extensiva* are long and extend almost at right angles from the tests (Duxbury, 1977), while in *M. tetracantha* the horns bend downwards (Gocht, 1957). Furthermore, *M. extensiva* in contrast to *M. tetracantha* show a distinct plate differentiation at the lateral edge (Helby, 1987).

Spitsbergen-this study. In the material encountered in the present study we observe transitional forms between *M. extensiva* and *M. tetracantha.* Some of these forms resemble *M. tetracantha* in their general outline, but on one or both lateral horns, we observe a distinct plate differentiation, a feature typical for *M. extensiva* (Fig. 7g). We observe the earliest record of *M. tetracantha* below the FO of *E. hauterivianum* (Fig. S1) but in sections with high dinocyst diversity and high relative abundance, the FO of *M. tetracantha* is observed within the range of *E. hauterivianum* (Figs S1, S2, S6, and 4)

9.e. Stratigraphic range of *Nelchinopsis kostromiensis* (Vozzhennikova, 1967) Wiggins, 1972

Figs 4m,n

In the majority of existing studies of the North Sea Basin (Fig. 7) the range of this species is limited to the upper lower Valanginian–upper Hauterivian (Costa & Davey, 1992; Duxbury, 2001) or to the Hauterivian (Davey, 1982; Heilmann-Clausen, 1987). In North-East Greenland the taxon first occurring in the middle late Valanginian and is not observed above the early to late Hauterivian *N. kostromiensis* Subzone (Nøhr-Hansen, 1993; Nøhr-Hansen, Piasecki & Alsen this issue). Some studies, reports the FO of *N. kostromiensis* as early as at the early–late Valanginian boundary (Bailey, 2019) and its LO in the earliest Barremian (Bailey, 2019). However, the Hauterivian–Barremian boundary in Bailey (2019) is dated as 130 Ma so it is slightly younger than in the Geological Time Scale 2016 where it is dated as 130.8 Ma (Ogg, Ogg & Gradstein, 2016). In the Svedrup Basin, Arctic Canada *N. kostromiensis* was observed together with *Gochteodinia villosa* in the middle-late late Valanginian succession (Davies, 1983). In some older studies *N. kostromiensis* was reported from the earliest Barremian (Heilmann-Clausen, 1987; Smelror *et al.*, 1998), from the *Simbirskites variabilis* ammonite zone. Today the zone is considered to be Hauterivian (Ogg, Ogg & Gradstein, 2016).

Spitsbergen – this study. The FO and LO of *N. kostromiensis* are important stratigraphic events within the Rurikfjellet Formation. The range of *N. kostromiensis* virtually spans the entire unit at the three outcrops and in the DH5R core. Applying the age constraint based on the range of *E. hauterivianum*, the FO of *N. kostromiensis* in Spitsbergen is an early Valanginian event, observed in the lower part of the Rurikfjellet Formation. The LO of *N. kostromensis* is observed in the upper part of the Rurikfjellet Formation and is probably of latest Hauterivian – earliest Barremian age.

9.f. FO of *Odontochitina nuda* (Gocht, 1957) Dörhöfer & Davies, 1980

Fig. 5e

The holotype of *O. nuda* was described from the upper Hauterivian (Gocht, 1957). Other studies from Europe and Canada also suggest a Hauterivian to Barremian stratigraphic range for the taxon (see discussion in Nøhr-Hansen, 1993), Fig. 7. In North-East Greenland *O. nuda* is restricted to the uppermost lower Barremian to lower Aptian (Nøhr-Hansen, 1993). In the Barents Sea the taxon was reported from early Barremian strata by Århus (in Århus *et al.* 1990), but notably this study was carried out only on a Berriasian to lower Barremian succession. Therefore, the youngest occurrence of the taxon in the Barents Sea is unknown.

Spitsbergen – this study. *O. nuda* is restricted to the Helvetiafjellet Formation. The FO is observed within the middle (the DH2 core) or the upper (the Ullaberget

outcrop section) part of the formation. The most probable time span for the taxon in Spitsbergen is Barremian to early Aptian.

9.g. FO of *Oligosphaeridium abaculum* Davey, 1979

Fig. 5f

The holotype of *O. abaculum* was described by Davey (1979) from a Barremian succession from the northern North Sea. In his study, Davey mentioned that abundant *O. abaculum* was found in the same sample as *Odontochitina operculata*, which has its first stratigraphic occurrence in the Barremian e.g. (Nøhr-Hansen, 1993; Bailey, 2019). The common occurrence of *O. abaculum* in the upper Hauterivian was reported in the UK and the Norwegian sectors of the North Sea Basin by Bailey (2019). Notably, Costa & Davey (1992) reported that in the UK sector of the North Sea Basin *O. abaculum* has a stratigraphic range from the upper Hauterivian to lower Barremian. However, the post-Hauterivian–Barremian? age was suggested by these authors because they considered the *Simbirskites variabilis* ammonite zone as Barremian. Recently the FO of *O. abaculum* was recorded from the uppermost lower Barremian in North-East Greenland by Nøhr-Hansen, Piasecki & Alsen (this issue).

Spitsbergen – this study. Rare to common (<1% and 1-30% of the total dinocyst assemblage) occurrences of *O.abaculum* are observed from all sites spanning the Rurikfjellet Formation. However, in contrast to the North Sea and North-East Greenland, in Spitsbergen the taxon appears in the Valanginian, i.e. much earlier than in the two

other regions (Fig. 7). We consider the FO of *O. abaculum* as an intra-late Valanginian event. The diachroneity in the event (Fig. 7) would suggest that the appearance of *O. abaculum* is dependent on the local environmental changes.

9.h. FO of *Oligosphaeridium* complex (White, 1842) Davey & Williams, 1966b

Fig. 5h

The FO of *O. complex* is an important marker for the base Valanginian in the North Sea Basin and the Svedrup Basin, Arctic Canada (Davies, 1983; Costa & Davey, 1992; Duxbury, 2001; Bailey, 2019). From North-East Greenland, Nøhr-Hansen, Piasecki & Alsen (this issue) recently recorded the FO of *O. complex* from the *Peregrinus albidum* ammomite zone, which is uppermost Berriasian in age [or lower Valanginian according to Ogg, Ogg & Gradstein (2016)]. On Andøya (Arctic Norway), the oldest record of *O. complex* is observed within beds assigned to the *Buchia inflata-Buchia keyserlingi* zones dated as Early Valanginian (Århus et. 1986).*Spitsbergen – this study*. In our material the taxon is present in virtually all samples. In the oldest part of the record, the taxon is often characterised by a small central body size and very tilted, long processes. The processes terminations often have a “palm-like” appearance (Fig. 5j). We consider the FO of *O. complex* as a marker for the base of the Valanginian. However, considering the recent study from North-East Greenland it is possiible that this event is slightly older (Nøhr-Hansen, Piasecki & Alsen this issue).

9.i. LO of *Palaecysta palmula* (Davey, 1982b) Williams & Fensome, 2016

Fig. 5k

In the UK sector of the Central North Sea Basin the LO of *P. palmula* is observed in the middle lower Valanginian (Duxbury, 2001; Bailey, 2019) while in the Danish sector the LO is probably slightly younger, within the lower upper Valanginian (Davey, 1982; Heilmann-Clausen, 1987), Fig. 7.

Spitsbergen – this study. In the present study *P. palmula* is observed in the basal part of the Rurikfjellet Formation in the Myklegardfjellet outcrop section.

9.j. Stratigraphic range of *Pseudoceratium anaphrissum* (Sarjeant, 1966c) Bint, 1986

Figs 5m–o

The taxon has a remarkably short range, limited to the Barremian, primarily to the lower Barremian (Fig. 7). In the high Arctic the taxon has also been observed in the Hauterivian (Fig. 7). The Barremian record of *P. anaphrissum* is very well known from the Barents Sea (Århus *et al.*, 1990), Arctic Norway (Thusu, 1978), offshore south Norway (Costa, 1981), North-East Greenland (Nøhr-Hansen, 1993), England (e.g. Sarjeant 1966, Duxbury 1980), Germany (Prössl, 1990) and the North Sea Basin (Heilmann-Clausen, 1987; Costa & Davey, 1992; Bailey, 2019). Notably, in Arctic

Norway a common occurrence of *P. anaphrissum* was found in a sample referred to upper Hauterivian – lower Barremian (Århus, Verdenius and Birkelund, 1986). In North-East Greenland, and possibly also in the UK and the Norwegian sector of the North Sea Basin, the species is abundant in a narrow interval in the middle part of its range (Nøhr-Hansen, 1993; Bailey, 2018), see also summary Fig. 7.

Spitsbergen – this study. In the present study *P. anaphrissum* is present in the uppermost part of the Rurikfjellet Formation (Ullaberget) and the Helvetiafjellet Formation (DH2 and Ullaberget). The taxon is rare (< 1%), badly preserved and incomplete (Figs 5m-o). All observed specimens have clearly visible antapical lobes and lateral buldges, and with no operculum. Specimens observed in DH2 and Ullaberget are covered by short spines and processes (Figs 5n-o). Due to a poor preservational state, the ornamentation of the specimen observed in the topmost sample from the Bohemanflya outcrop section (Fig. 8m) is difficult to establish and therefore the specimen is referred to *P. anaphrissum* questionably.

In the middle and upper part of the Rurikfjellet Formation we found the common occurrence of dinocysts which we referred to *Cleistosphaeridium diversispinosum* (Figs 6g, 6i). The ornamentation may resemble *P. anaphrissum,* but the outline is more typical for the genus *Circulodinium.*

9.k. LO of *Sirmiodinium grossii* Alberti, 1961

Figs 6e,f

The LO of *S. grossii* marks the top of the Barremian (e.g. Bailey, 2019). In North-East Greenland the youngest record of the taxon is observed within the lowermost Aptian (Nøhr-Hansen, 1993). More details concerning the distribution of the taxon in the Boreal and the European Boreal Realm is shown on Fig. 7.

Spitsbergen – this study. We observe *S. grossii* in both the Rurikfjellet and Helvetiafjellet formations. The taxon is present in virtually all samples analysed in this study.

9.l. FO of *Subtilisphaera perlucida* (Alberti, 1959b) Jain & Millepied, 1973

Fig. 6g

The majority of existing records from the Boreal and European Boreal Realm suggest that *S. perlucida* appeared in the early Barremian (Heilmann-Clausen, 1987; Nøhr-Hansen, 1993). In the DH1 core the FO of *S. perlucida* was observed within the Helvetiafjellet Formation and dated as Barremian – Aptian (Midtkandal *et al.*, 2016). Some records suggest however that the taxon appeared in the late Hauterivian (Fig. 7).

Spitsbergen – this study. The taxon is observed in the uppermost part of the Rurikfjellet Formation (Ullaberget) and occurs consistently in the Helvetiafjellet Formation (Ullaberget and the DH2 core).

9.m. LO of *Tubotuberella apatela* (Cookson & Eisenack, 1960b) Ioannides et al., 1977

Figs 6 i-j

In the majority of studies on the North Sea the LO of *T. apatela* occurs approximately within the middle lower Valanginian (Fig. 7) and is considered synchronous with (Bailey, 2019) or slightly younger than (Duxbury, 2001) the LO of *P. palmula.* In the Barents Sea *T. apatela* was not observed in the post-Ryazanian strata, but this may be biased by the fact that the Valanginian succession is devoid of palynomorphs (Århus *et al.*, 1990). Numerous studies report *T. apatela* from the upper Valanginian (Davies, 1983; Århus, 1988) or even Hauterivian (Piasecki, 1979; Davey, 1982; Heilmann-Clausen, 1987) deposits. These studies report that the last persistent occurrence of *T. apatela* occurs within the early Valanginian. In Spitsbergen and North-East Greenland the post-Valanginian occurrence of the taxon is considered as reworked (Århus, 1988; Nøhr-Hansen, 1993).

Spitsbergen – this study. In the present study *T. apatela* is present within the lower to middle part of the Rurikfjellet Formation. We observe that the LO on Spitsbergen is diachronous. In the Myklegardfjellet outcrop section we apply the LO of persistent *T. apatela* as the marker for the top of early Valanginian (Fig. 8). *T. apatela*, in contrast to *Tubotuberella rhombiformis*, has a distinctive apical horn (on both epitheca, and hypotheca), and lacks tabulation. These two features are clearly visible in virtually all specimens observed in this study.

Acknowledgements

This research was carried out within the LoCrA consortium (https://wp.ux.uis.no/locra), generously sponsored by 22 industry partners. Thanks are extended to Annette Ryge, Charlotte Olsen, and Dorthe Samuelsen (GEUS) for preparation of palynological slides. S.-A. Grundvåg acknowledges funding from the ARCEx project (Research Centre for Arctic Petroleum Exploration) which is funded by the Research Council of Norway (grant number 228107). Figures 8, 9, and S1-S6 were prepared using the StrataBugs v2.0 charts. We thank reviewers Wiesława Violka Radmacher and Kari Grøsfjeld as well as editor Jennifer Galloway for valuable comments and suggestions, which improved this manuscript.

Declaration of Interest

The authors declare no conflicts of interest.

Figure captions

Figure 1. Stratigraphic cross-section showing the regional development of the Upper Jurassic to Lower Cretaceous Adventdalen Group on Spitsbergen. Modified after Alsen *et al.* (this issue). White bars show the time span for each of the studied sites: three onshore cores DH1, DH2, DH5R, and three outcrop sections: Bohemanflya (BOH), Ullaberget (UL), and Myklegardfjellet (MYK).

Figure 2. (**A).** Black dots mark the positions of the studied sites: Bo – Bohemanflya, Ul – Ullaberget, My – Myklegardfjellet outcrop sections. Paleogeography of Spitsbergen from the Valanginian to early Aptian (after Grundvåg & Olaussen, 2017; Grundvåg *et*

al., 2017) (**B**) Palaeogeography during the deposition of the Wimanfjellet Member; (**C**) Palaeogeography during the deposition of the Kikutodden Member; (**D**) Paleogeography during the earliest Barremian - deposition of the Festningen Member.

Figure 3. Photographs of the most characteristic dinoflagellate cysts observed in the Rurikfjellet and Helvetiafjellet formations in the present study. Scale bars on all photographs represent 20 µm. MC – microscope coordinates with the A-point of 0.4×90.3 (*X*M1 × *Y*M1). For details, see Śliwińska (2019).

(a) a dinocyst, Bohemanflya outcrop section, level 99.29 m, sample 26291-7, MC 102 x 42.2

(b) *Apteodinium spongiosum*, high focus, (c) low focus, Bohemanflya outcrop section, level 25.00 m, sample 28450-9, MC 25 x 108.7

(d) *Apteodinium spongiosum* very dark, Myklegardfjellet outcrop section, level 30.00 m, sample 27007-6, MC 32 x 109.1

(e) *Apteodinium spongiosum*, Myklegardfjellet outcrop section, level 120.00 m, sample 27013-9; MC 51.4 x 105.5

(f) *Atopodinium haromense*; Myklegardfjellet outcrop section, level 120.00 m, sample 27013-9; MC 42.7 x 102.3

(g) *Circulodinium distinctum*, Myklegardfjellet outcrop section, level 105.00 m, sample 27012-6; MC 29.3 x 91.6

(h) *Circulodinium distinctum*, Myklegardfjellet outcrop section, level 120.00 m, sample 27013-9; MC 21 x 104.5

(i) *Circulodinium distinctum*, Myklegardfjellet outcrop section, level 120.00 m, sample 27013-9; MC 17.5 x 105.5

(j) *Circulodinium distinctum*, Bohemanflya outcrop section, level 28.00 m, sample 28449-8; MC 44.7 x 96.7

(k) *Dissiliodinium acmeum*, Myklegardfjellet outcrop section, level 7.00 m, sample 27005-4; MC 37.2 x 99.4

(l) *Endoscrinium* sp.1 Bohemanflya outcrop section, level 25.00 m, sample 28450-9 ; MC 25.5 x 110

(m) *Discorsia nannus*, Myklegardfjellet outcrop section, level 120.00 m, sample 27013-9; MC 49 x 103.3

(n) *Dingodinium cerviculum*, Myklegardfjellet outcrop section, level 75.00 m, sample 27010-4; MC 47 x 108.5

(o) *Endoscrinium hauterivianum*, Bohemanflya outcrop section, level 36.00 m, sample 28448-7, MC 33.8 x 102.2

(p) *Endoscrinium hauterivianum*, Myklegardfjellet outcrop section, level 120.00 m, sample 27013-9; MC 42 x 102.4

Figure 4. Photographs of the most characteristic dinoflagellate cysts observed in the Rurikfjellet and Helvetiafjellet formations in the present study. Scale bars on all photographs represent 20 μm. The figure in colour is available on the web version of

this paper. MC – microscope coordinates with the A-point of 0.4×90.3 (*X*M1 × *Y*M1). For details, see Śliwińska (2019).

(a) *Gochteodinia villosa* subsp. *multifurcata*, Myklegardfjellet outcrop section, level 15.00 m, sample 27006-5, MC 36.3 x 114

(b) *Gochteodinia villosa*, DH5R core, depth 350.00 m, sample 26197-6; MC 22.5 x 96.2

(c) *Gochteodinia villosa* subsp. *multifurcata*, Myklegardfjellet outcrop section, level 15.00 m, sample 27006-5; MC 36 x 107

(d) *Muderongia tetracanta*, Bohemanflya outcrop section, level 127.50 m, sample 26290-8, MC 44 x 110.6

(e) *Muderongia australis*, Myklegardfjellet outcrop section, level 120.00 m, sample 27013-9; MC 31.4 x 108.5

(f) *Muderongia simplex*, Myklegardfjellet outcrop section, level 105.00 m, sample 27012-6; MC 33 x 105.8

(g) a transitional form between *Muderongia tetracanta* and *Muderongia extensiva*, Bohemanflya outcrop section, level 46.00 m, sample 26293-5, MC 24.5 x 111

(h) *Muderongia extensiva,* Bohemanflya outcrop section, level 46.00 m, sample 26293-7; MC 18.5 x 108.4

(i) *Isthmocystis distincta*, Myklegardfjellet outcrop section, level 7.00 m, sample 27005-4; MC 28 x 102.3

(j) *Kleithriasphaeridium eoinodes*, Myklegardfjellet outcrop section, level 90.00 m, sample 27011-8; MC 25.2 x 103

(k) *Kiokansium unituberculatum*, Bohemanflya outcrop section, level 127.50, sample 26290-6; MC 31x107.3

(l) *Meiourogonyaulax stoveri*, DH5R core, depth 258.00 m, sample 26194-5; MC 24 x 107.8

(m) poorly preserved *Nelchinopsis kostromiensis,* Bohemanflya outcrop section, level 99.29 m, sample 26291-7; MC 52.4 x 109

(n) *Nelchinopsis kostromiensis,* Bohemanflya outcrop section, level 55.25 m, sample 26292-7; MC 51.5 x 95.5

(o) *Nyktericysta? pannosa*, Bohemanflya outcrop section, level 99.29 m, sample 26291-7; MC 43 x 102.7

(p) *Nyktericysta? pannosa*, Bohemanflya outcrop section, level 127.50 m, sample 26290-8; MC 50.2 x 100

Figure 5. Photographs of the most characteristic dinoflagellate cysts observed in the Rurikfjellet and Helvetiafjellet formations in the present study. Scale bars on all photographs represent 20 µm. The figure in colour is available on the web version of this paper. MC – microscope coordinates with the A-point of 0.4×90.3 (*X*M1 × *Y*M1). For details, see Śliwińska (2019).

(a) *Oligosphaeridium poculum*, DH5R core, depth 320.00 m, sample 26196-7; MC 58.2 x 97.1

(b) questionable *Escharisphaeridia rudis*, DH5R core, depth 288.00 m, sample 26195-7; MC 36.7 x 112.5

(c) *Phoberocysta neocomica*, Myklegardfjellet outcrop section, level 90.00 m, sample 27009-6; MC 24.3 x 113.8

(d) *Rhynchodiniopsis aptiana*, Bohemanflya outcrop section, level 5.00 m, sample 28453-7, MC 31.7 x 101

(e) *Odontochitina nuda*, DH2 core, depth 141.80 m, sample 26510-9; MC 42 x 105.2

(f) *Oligosphaeridium abaculum*, Myklegardfjellet outcrop section, level 75.00 m, sample 27010-5; MC 48.5 x 105.5

(g) *Rhynchodiniopsis aptiana*, Myklegardfjellet outcrop section, level 105.00 m, sample 27012-6; MC 20.3 x 107.5

(h) *Oligosphaeridium complex* with “palm-like” terminations of processes, DH1, depth 258.90 m, sample 26285-7; MC 32.8 x 97.1

(i) *Oligosphaeridium asterigerum*, Bohemanflya outcrop section, level 99.29 m, sample 26291-7, MC 44.7 x 94.3

(j) *Pseudoceratium pelliferum*, Bohemanflya outcrop section, level 36.00 m, sample 28448-7, MC 37 x 106.5

(k) *Palaecysta palmula*, Myklegardfjellet outcrop section, level 0.05 m, sample 27004-8, MC 53 x 107.5

(l) *Cyclonephelium cuculliforme* sensu Århus 1990, Myklegardfjellet outcrop section, level 15.00, sample 27006-3; MC 30.2 x 101

(m) questionable *Pseudoceratium anaphrissum* Bohemanflya outcrop section, level 132.63 m, sample 26289-8; MC 37.8 x 95.5. Shown also in Figure 15.P in Grundvåg *et al.*, (2019).

(n) *Pseudoceratium anaphrissum*, Ullaberget outcrop section, level 104.00m, sample 28482-7; MC 40.6 x 111.8

(o) questionable, poorly preserved *Pseudoceratium anaphrissum*, DH2 core, depth 149.50 m, sample 26511-11; MC 34.5 x 110.5. Shown also in Figure 15.H in Grundvåg *et al.*, (2019).

Figure 6. Photographs of the most characteristic dinoflagellate cysts observed in the Rurikfjellet and Helvetiafjellet formations in the present study. Scale bars on all photographs represent 20 µm. The figure in colour is available on the web version of this paper. MC – microscope coordinates with the A-point of 0.4×90.3 (*X*M1 × *Y*M1). For details, see Śliwińska (2019).

(a) *Stanfordella fastigiata*, Myklegardfjellet outcrop section, level 30.00 m, sample 27007-6; MC 50.4 x 103.5

(b) *Stanfordella ordocava*, Myklegardfjellet outcrop section, level 15.00 m, sample 27006-5; MC 31.6 x 111

(c) *Stanfordella ordocava*, DH5R core, depth 380.00 m, sample 26198-6; MC 55.5 x 102.4

(d) Spiniferites sp. 1, DH5R core, depth 194.00 m, sample 26192-7; MC 36.9 x 102

(e) *Sirmiodinium grossii*, Myklegardfjellet outcrop section, level 30.00 m, sample 27007-6; MC 30.3 x 104.2

(f) *Sirmiodinium grossii*, DH1, depth 258.90 m, sample 26285-7; MC 29.4 x 109

(g*) Subtilisphaera perlucida*, DH2 core, depth 186.55 m, sample 26513-9; MC 36.7 x 92.6. Shown also in Figure 15.G in Grundvåg *et al*., (2019).

(h) *Spiniferites*? DH5R core, depth 194.00 m, sample 26192-7; MC 50.8 x 101.2

(i) *Tubotuberella apatela*, Myklegardfjellet outcrop section, level 30.00 m, sample 27007-6; MC 30.6 x 105

(j) *Tubotuberella apatela*, Myklegardfjellet outcrop section, level 0.05 m, sample 27004-8; MC 34.5 x 109.4

(k) *Tubotuberella apatela*, DH2 core, depth 232.00 m, sample 26516-9; MC 19.4 x 93.3

(l) *Tubotuberella* sp. DH5R core, depth 380.0 m, sample 26198-6; MC 48 x 98.7

(m) *Wallodinium luna*, DH5R core, depth 350.0 m, sample 26197-6; MC 36.5 x 102.4

(n) *Wrevittia perforobtusa*, DH5R core, depth 194.00 m, sample 26192-7; MC 29.9 x 102.6

(o) *Wrevittia perforobtusa*, Bohemanflya outcrop section, level 55.25 m, sample 26292-8, MC 50.3 x 101.7

(p) *Wrevittia perforobtusa*, Bohemanflya outcrop section, level 36 m, sample 28448-7, MC 40.5 x 98.6

Figure 7. The stratigraphic ranges and/or first and last occurrences of the age diagnostic dinoflagellate cysts (dinocysts) from the Boreal and European Boreal Realm,

and the key events recognised in this study (to the right). Key dinocyst events in Spitsbergen: primary markers (black), secondary markers (grey).

The figure shows a compilation of the most characteristic dinocysts from the Rurikfjellet and Helvetiafjellet formations discussed in the present study. Heilmann-Clausen (1987), Costa & Davey (1992), and Duxbury (2001) plotted the dinocysts ranges against the ammonite zonation (marked with asterix). All these authors considered the *Simbirskites variabilis* ammonite zone as earliest Barremian, whilst today it is considered to be Hauterivian (Ogg, Ogg & Gradstein, 2016). Nøhr-Hansen, Piasecki & Alsen (this issue) updated the zonation proposed previously by Nøhr-Hansen (1993), and provided ages in GTS2016. Note that the study by Davey (1982) does not cover sediments younger than early-?late Hauterivian, while the study by Davies (1983) does not cover sediments younger than late Valanginian.

Figure 8. The spatial distribution of the age diagnostic (colour code) and secondary dinocyst events (black) within the Rurikfjellet Formation. The correlation between the Bohemanflya, the DH5R core, and the Myklegardfjellet outcrop section, i.e. from NW to SE.

Figure 9. The spatial distribution of the age diagnostic dinocyst events within the Helvetiafjellet Formation. The correlation between the Ullaberget outcrop section and the DH2 core.

online Supplementary Material at http://journals.cambridge.org/geo

This file contains range charts with the quantitative data of the palynomorphs recognised in this study. The palynomorphs are arranged after the first occurrence (FO), R – reworked, DC – dinocyst, AC – acritarch, MP – palynomorph

Figure S1. Distribution of dinocysts in the Bohemanflya outcrop section

Figure S2. Distribution of dinocysts in the Myklegardfjellet outcrop section

Figure S3. Distribution of dinocysts in the Ullaberget outcrop section

Figure S4. Distribution of dinocysts in the DH1 well

Figure S5. Distribution of dinocysts in the DH2 well

Figure S6. Distribution of dinocysts in the DH5R well

References

Alsen, P. *et al.* (2019) 'An Early Cretaceous stratigraphic marker fossil in the High Arctic – the belemnite Arctoteuthis bluethgeni', *Geological Magazine*.

Århus, N. (1988) 'Palynostratigraphy of some Bathonian – Hauterivian sections in the Arctic with emphasis on the Janusfjellet Formation type section, Spitsbergen. Confidential report No. 88.084', p. 139.

Århus, N. *et al.* (1990) 'Systematic palaeontology and biostratigraphy of two Early Cretaceous condensed sections from the Barents Sea', *Polar Research*, 8(2), pp. 165–194. doi: 10.1111/j.1751-8369.1990.tb00383.x.

Århus, N. (1991) 'Dinoflagellate cyst stratigraphy of some Aptian and Albian sections from North Greenland, southeastern Spitsbergen and the Barents Sea', *Cretaceous*

Research, 12(3), pp. 209–225. doi: 10.1016/0195-6671(91)90035-B.

Århus, N. (1992) 'Some dinoflagellate cysts from the lower cretaceous of spitsbergen', *Grana*, 31(4), pp. 305–314. doi: 10.1080/00173139209429453.

Århus, N., Verdenius, J. and Birkelund, T. (1986) 'Biostratigraphy of a Lower Cretaceous section from Sklinnabanken, Norway, with some comments on the Andøya exposure', *Norsk Geologisk Tidsskrift*, 66, pp. 17–43.

Bailey, D. (2019) *Early Cretaceous Zonation (www.biostrat.org.uk/EK Zones 2011postcon.pdf)*. Available at: http://www.biostrat.org.uk/EK Zones 2011postcon.pdf (Accessed: 15 May 2019).

Basov, V. A. *et al.* (2009) *Geological History of the Barents Sea*. Edited by M. Smelror et al. Trondheim: Norges geologiske undersøkelse (Geological Survey of Norway). Available at: https://issuu.com/ngu_/docs/atlas_-%0A_geological_history_of_the_b/1?e=3609664/902604%0A.

Birkenmajer, K., Pugaczewska, H. and Wierzbowski, A. (1979) 'The Janusfjellet Formation (Jurassic-Lower Cretaceous) at Myklegardfjellet, East Spitsbergen', *Palaeontologia Polonica*, 43, pp. 107–140.

Bjærke, T. (1978) 'Mesozoic palynology of Svalbard III. Dinoflagellates from the Rurikfjellet Member, Janusfjellet Formation (Lower Cretaceous) of Spitsbergen', *Palinologia, numero extraord.*, pp. 69–93.

Bjærke, T. (1980) 'Preprint: Mesozoic Palynology of Svalbard VI. Palynological zonation of the Upper Triassic, Jurassic and Lower Cretaceous sequence in Svalbard', pp. 1–74.

Bjærke, T. and Thusu, B. (1976) 'Cretaceous Palynomorphs from Spitsbergenbanken

NW Barents Shelf.', *Norsk Polarinstitut Årbok 1974*, pp. 258–262.

Bottini, C. *et al.* (2015) 'Climate variability and ocean fertility during the Aptian Stage', *Climate of the Past*. doi: 10.5194/cp-11-383-2015.

Bottini, C. and Erba, E. (2018) 'Mid-Cretaceous paleoenvironmental changes in the western Tethys', *Clim. Past*. Copernicus Publications, 14(8), pp. 1147–1163. doi: 10.5194/cp-14-1147-2018.

Braathen, A. *et al.* (2012) 'The Longyearbyen CO2 lab of Svalbard, Norway - initial assessment of the geological conditions for CO2 sequestration', *Norsk Geologisk Tidsskrift*. doi: 10.1095/biolreprod.111.094433.

Brideaux, W. W. (1977) 'Taxonomy of Upper Jurassic-Lower Cretaceous Microplankton from the Richardson Mountains, District of Mackenzie, Canada', *Geological Survey of Canada, Bulletin*, 281, pp. 1–89. doi: 10.4095/102868.

Corfu, F. *et al.* (2013) 'U-Pb geochronology of cretaceous magmatism on Svalbard and Franz Josef Land, Barents Sea large igneous province', *Geological Magazine*, 150(6), pp. 1127–1135. doi: 10.1017/S0016756813000162.

Costa, L. (1981) 'Palynostratigraphy, Upper Cretaceous to Lower Cretaceous in the wells 2/7-1 and 2/7-3', in Ofstad, K. (ed.) *The Eldfisk area*. Norwegian Petroleum Dir. Pap., pp. 1–34.

Costa, L. and Davey, R. J. (1992) 'Dinoflagellate cysts of the Cretaceous System', in Powell, A. . (ed.) *A stratigraphic index of dinoflagellate cysts*. London: British Micropalaeontological Society Publication Series, Chapman and Hall, pp. 99–153.

Davey, R. J. (1979a) 'The stratigraphic distribution of dinocysts in the Portlandian (latest

Jurassic) to Barremian (early Cretaceous) of northwest Europe', *AASP Contributions Series*, 5B, pp. 49–81.

Davey, R. J. (1979b) 'Two new Early Cretaceous dinocyst species from the northern North Sea', *Palaeontology*, 22, pp. 427–437.

Davey, R. J. (1982) 'Dinocyst stratigraphy of the latest Jurassic to Early Cretaceous of the Haldager No. 1 borehole, Denmark', *Danmarks Geologiske Undersøgelse*, Series B(6), pp. 1–57.

Davey, R. J. (1988) 'Palynological zonation of the Lower Cretaceous, Upper and uppermost Middle Jurassic in the northwestern Papuan Basin of Papua New Guinea', *Geological Survey of Papua New Guinea, Memoir*, 13, pp. 1–77.

Davies, E. H. (1983) 'The Dinoflagellate Oppel-zonation of the Jurassic-Lower Cretaceous Sequence in the Sverdrup Basin, Arctic Canada', *Geological Survey of Canada Bulletin*. Geological Survey of Canada Bulletin (359): 1-59, 359, pp. 1–59.

Dietmar Müller, R. and Spielhagen, R. F. (1990) 'Evolution of the Central Tertiary Basin of Spitsbergen: towards a synthesis of sediment and plate tectonic history', *Palaeogeography, Palaeoclimatology, Palaeoecology*, 80(2), pp. 153–172. doi: 10.1016/0031-0182(90)90127-S.

Ditchfield, P. W. (1997) 'High northern palaeolatitude Jurassic-Cretaceous palaeotemperature variation: New data from Kong Karls Land, Svalbard', *Palaeogeography, Palaeoclimatology, Palaeoecology*, 130, pp. 163–175. doi: 10.1016/S0031-0182(96)00054-5.

Dörr, N. *et al.* (2012) 'Late Mesozoic-Cenozoic exhumation history of northern Svalbard

and its regional significance: Constraints from apatite fission track analysis', *Tectonophysics*, 514–517, pp. 81–92. doi: 10.1016/j.tecto.2011.10.007.

Duxbury, S. (1977) 'A palynostratigraphy of the Berriasian to Barremian of the Speeton Clay of Speeton, England', *Palaeontographica Abteilung B*, 160(1–3), pp. 17–67.

Duxbury, S. (1980) 'Barremian phytoplankton from Speeton, east Yorkshire', *Palaeontographica Abteilung B*, 173(4–6), pp. 107–146.

Duxbury, S. (2001) 'A palynological zonation scheme for the Lower Cretaceous - United Kingdom sector, central North Sea', *Neues Jahrbuch fuer Geologie und Palaeontologie Abhandlungen*, 219(1–2), pp. 95–137.

Dypvik, H. *et al.* (1991) 'The Janusfjellet Subgroup (Bathonian to Hauterivian) on central Spitsbergen: a revised litostratigraphy', *Polar Research*, 9(1).

Dypvik, H., Nagy, J. and Krinsley, D. H. (1992) 'Origin of the Myklegardfjellet Bed, a basal Cretaceous marker on Spitsbergen', *Polar Research*, 11(1), pp. 21–31. doi: 10.1111/j.1751-8369.1992.tb00409.x.

Erbacher, J., Thurow, J. and Littke, R. (1996) 'Evolution patterns of radiolaria and organic matter variations: A new approach to identify sea-level changes in mid-Cretaceous pelagic environments', *Geology*, 24(6), pp. 499–502. doi: 10.1130/0091-7613(1996)024<0499:EPORAO>2.3.CO;2.

Galloway, J. M. *et al.* (2015) 'Early Cretaceous vegetation and climate change at high latitude: Palynological evidence from Isachsen Formation, Arctic Canada', *Cretaceous Research*, 56, pp. 399–420. doi: 10.1016/j.cretres.2015.04.002.

Gjelberg, J. and Steel, R. J. (1995) 'Helvetiafjellet formation (Barremian-Aptian),

Spitsbergen: Characteristics of a transgressive succession', *Norwegian Petroleum Society Special Publications*. doi: 10.1016/S0928-8937(06)80087-1.

Gocht, H. (1957) 'Mikroplankton aus dem nordwestdeutschen Neokom (Teil I)', *Paläontologische Zeitschrift*, 31, pp. 163–185.

Gradstein, F. M., Kaminski, M. A. and Agterberg, F. P. (1999) 'Biostratigraphy and paleoceanography of the Cretaceous seaway between Norway and Greenland', *Earth Science Reviews*, 46, pp. 27–98. doi: 10.1016/S0012-8252(99)00018-5.

Grøsfjeld, K. (1991) 'Palynological age constraints on the base of the Helvetiafjellet Formation (Barremian) on Spitsbergen', *Polar Research*, 11(1), pp. 11–19. doi: 10.1111/j.1751-8369.1992.tb00408.x.

Grundvåg, S.-A. *et al.* (2017) 'The Lower Cretaceous succession of the northwestern Barents Shelf: Onshore and offshore correlations', *Marine and Petroleum Geology*, 86, pp. 834–857. doi: 10.1016/j.marpetgeo.2017.06.036.

Grundvåg, S.-A. *et al.* (2019) 'Sedimentology and palynology of the Lower Cretaceous succession of central Spitsbergen: integration of subsurface and outcrop data', *Norwegian Journal of Geology*, 99(2). doi: 10.17850/njg006.

Grundvåg, S.-A. and Olaussen, S. (2017) 'Sedimentology of the Lower Cretaceous at Kikutodden and Keilhaufjellet, southern Spitsbergen: Implications for an onshore-offshore link', *Polar Research*. doi: 10.1080/17518369.2017.1302124.

Hammer, Ø. *et al.* (2018) 'Comment on "Redox conditions, productivity, and volcanic input during deposition of uppermost Jurassic and Lower Cretaceous organic-rich siltstones in Spitsbergen, Norway" by Rakocinski et al. (2018)', *Cretaceous Research*,

96, pp. 241–243. doi: 10.1016/j.cretres.2018.02.014.

Harland, W. B. (1997) 'The geology of Svalbard', *Journal of the Geological Society of London*, 17, p. 521.

Heilmann-Clausen, C. (1987) 'Lower Cretaceous dinoflagellate biostratigraphy in the Danish Central Trough', *Geological Survey of Denmark and Greenland Bulletin*, A(17), pp. 1–89.

Helby, R. (1987) 'Muderongia and related dinoflagellates of the latest Jurassic to Early Cretaceous of Australasia', in Jell, P. A. (ed.) *Studies in Australian Mesozoic palynology*, pp. 297–336.

Henriksen, E. *et al.* (2011) 'Chapter 10 Tectonostratigraphy of the greater Barents Sea: implications for petroleum systems', *Geological Society, London, Memoirs*, 35(1), pp. 163 LP – 195. doi: 10.1144/M35.10.

Herrle, J. O. *et al.* (2015) 'Mid-Cretaceous High Arctic stratigraphy, climate, and Oceanic Anoxic Events', *Geology*, 43(5), pp. 403–406. doi: 10.1130/G36439.1.

Van Hinsbergen, D. J. J. *et al.* (2015) 'A paleolatitude calculator for paleoclimate studies', *PLoS ONE*, 10(6). doi: 10.1371/journal.pone.0126946.

Hochuli, P. A. *et al.* (1999) 'Episodes of high productivity and cooling in the early Aptian Alpine Tethys', *Geology*. doi: 10.1130/0091-7613(1999)027<0657:EOHPAC>2.3.CO;2.

Holden, J. C. (1970) 'Reconstruction of Pangaea ' breakup and dispersion of continents, Permian to Present', *Journal of Geographical Research*, 75(26), pp. 4939–4956. doi: 10.1029/JB075i026p04939.

Huber, B. T. *et al.* (2018) 'The rise and fall of the Cretaceous Hot Greenhouse climate',

Global and Planetary Change. Elsevier, 167, pp. 1–23. doi: 10.1016/j.gloplacha.2018.04.004.

Hurum, J. H., Roberts, A. J., *et al.* (2016) 'Bird or maniraptoran dinosaur? A femur from the Albian strata of Spitsbergen', *Palaeontologia Polonica*, 67, pp. 137–147. doi: 10.4202/pp.2016.67_137.

Hurum, J. H., Druckenmiller, P. S., *et al.* (2016) 'The theropod that wasn't: an ornithopod tracksite from the Helvetiafjellet Formation (Lower Cretaceous) of Boltodden, Svalbard', *Geological Society, London, Special Publications*, 434, pp. 189–206. doi: 10.1144/sp434.10.

Jenkyns, H. C. (2010) 'Geochemistry of oceanic anoxic events', *Geochemistry, Geophysics, Geosystems*, 11(3), pp. 1–30. doi: 10.1029/2009GC002788.

Jenkyns, H. C. *et al.* (2012) 'Warm Middle Jurassic-Early Cretaceous high-latitude sea-surface temperatures from the Southern Ocean', *Climate of the Past*, 8(1), pp. 215–225. doi: 10.5194/cp-8-215-2012.

Johnston, F. K. B., Turchyn, A. V. and Edmonds, M. (2011) 'Decarbonation efficiency in subduction zones: Implications for warm Cretaceous climates', *Earth and Planetary Science Letters*, 303(1), pp. 143–152. doi: 10.1016/j.epsl.2010.12.049.

Kairanov, B. *et al.* (2018) 'Lower Cretaceous tectonostratigraphic evolution of the northcentral Barents Sea', *Journal of Geodynamics*, 119, pp. 183–198. doi: 10.1016/j.jog.2018.02.009.

Koevoets, M. J. *et al.* (2018) 'Integrating subsurface and outcrop data of the middle jurassic to lower cretaceous agardhfjellet formation in central spitsbergen', *Norsk*

Geologisk Tidsskrift, 98(4), pp. 1–34. doi: 10.17850/njg98-4-01.

Koopmann, H. *et al.* (2014) 'The late rifting phase and continental break-up of the southern South Atlantic: the mode and timing of volcanic rifting and formation of earliest oceanic crust', *Geological Society, London, Special Publications*. doi: 10.1144/sp420.2.

Lebedeva, N. K. and Nikitenko, B. L. (1999) 'Dinoflagellate cysts and microforaminifera of the lower cretaceous yatria river section, subarctic ural, NW Siberia (Russia). Biostratigraphy, palaeoenvironmental and palaeogeographic discussion', *Grana*. doi: 10.1080/00173139908559222.

Leckie, R. M., Bralower, T. J. and Cashman, R. (2002) 'Oceanic anoxic events and plankton evolution: Biotic response to tectonic forcing during the mid-Cretaceous', *Paleoceanography*. doi: 10.1029/2001PA000623.

Lehmann, J. (2015) 'Ammonoid Paleobiology: From macroevolution to paleogeography', in Klug, C. et al. (eds) *Ammonoid Paleobiology: From macroevolution to paleogeography*. Springer, pp. 403–429. doi: 10.1007/978-94-017-9633-0.

Littler, K. *et al.* (2011) 'High sea-surface temperatures during the Early Cretaceous Epoch', *Nature Geoscience*. Nature Publishing Group, 4(3), pp. 169–172. doi: 10.1038/ngeo1081.

Løfaldi, M. and Thusu, B. (1976) 'Microfossils from the Janusfjellet Subgroup (Jurassic-Lower Cretaceous) at Agardhfjellet and Keilhaufjellet, Spitsbergen. A preliminary report', *Norsk Polarinstitut Årbok 1975*, pp. 69–77.

De Lurio, J. L. and Frakes, L. A. (1999) 'Glendonites as a paleoenvironmental tool: Implications for early Cretaceous high latitude climates in Australia', *Geochimica et*

Cosmochimica Acta. doi: 10.1016/S0016-7037(99)00019-8.

Marin, D. *et al.* (2017) 'Sequence stratigraphy and lateral variability of Lower Cretaceous clinoforms in the southwestern Barents Sea', *AAPG Bulletin*, 101(9), pp. 1487–1517. doi: 10.1306/10241616010.

Marín, D., Escalona, A., Grundvåg, S. A., Nøhr-Hansen, H., *et al.* (2018) 'Effects of adjacent fault systems on drainage patterns and evolution of uplifted rift shoulders: The Lower Cretaceous in the Loppa High, southwestern Barents Sea', *Marine and Petroleum Geology*. Elsevier, 94(November 2017), pp. 212–229. doi: 10.1016/j.marpetgeo.2018.04.009.

Marín, D., Escalona, A., Grundvåg, S. A., Olaussen, S., *et al.* (2018) 'Unravelling key controls on the rift climax to post-rift fill of marine rift basins: insights from 3D seismic analysis of the Lower Cretaceous of the Hammerfest Basin, SW Barents Sea', *Basin Research*, 30(4), pp. 587–612. doi: 10.1111/bre.12266.

McIntyre, D. J. and Brideaux, W. . W. (1980) 'Valanginian miospore and microplankton assemblages from the northern Richardson Mountains, District of Mackenzie', *Geological Survey of Canada, Bulletin*, 320, pp. 1–57.

Midtkanal, I. *et al.* (2008) 'Lower Cretaceous lithostratigraphy across a regional subaerial unconformity in spitsbergen: The Rurikfjellet and Helvetiafjellet Formations', in *Norsk Geologisk Tidsskrift*.

Midtkandal, I. *et al.* (2016) 'The Aptian (Early Cretaceous) oceanic anoxic event (OAE1a) in Svalbard, Barents Sea, and the absolute age of the Barremian-Aptian boundary', *Palaeogeography, Palaeoclimatology, Palaeoecology*, 463, pp. 126–135.

doi: 10.1016/j.palaeo.2016.09.023.

Midtkandal, I. and Nystuen, J. P. (2009) 'Depositional architecture of a low-gradient ramp shelf in an epicontinental sea: The lower Cretaceous of Svalbard', *Basin Research*. doi: 10.1111/j.1365-2117.2009.00399.x.

Midtkandal, I., Nystuen, J. P. and Nagy, J. (2007) 'Paralic sedimentation on an epicontinental ramp shelf during a full cycle of relative sea-level fluctuation; the Helvetiafjellet Formation in Nordenskiöld land, Spitsbergen', *Norsk Geologisk Tidsskrift*.

Mutterlose, J., Pauly, S. and Steuber, T. (2009) 'Temperature controlled deposition of early Cretaceous (Barremian-early Aptian) black shales in an epicontinental sea', *Palaeogeography, Palaeoclimatology, Palaeoecology*. doi: 10.1016/j.palaeo.2008.04.026.

Nikitenko, B. L. *et al.* (2008) 'Micropalaeontological and palynological analyses across the Jurassic-Cretaceous boundary on Nordvik Peninsula, Northeast Siberia', *Newsletters on Stratigraphy*, 42(3), pp. 181–222. doi: 10.1127/0078-0421/2008/0042-0181.

Nøhr-Hansen, H. (1993) *Dinoflagellate cyst stratigraphy of the Barremian to Albian, lower Cretaceous, North-East Greenland*. Bulletin. 166. Danmarks og Grønlands Geologiske Undersøgelse.

Nøhr-Hansen, H. and McIntyre, D. J. (1998) 'Upper Barremian to upper Albian (Lower Cretaceous) dinoflagellate cyst assemblages, Canadian Arctic archipelago', *Palynology*. doi: 10.1080/01916122.1998.9989506.

Nøhr-Hansen, H., Piasecki, S. and Alsen, P. (2019) 'A Cretaceous dinoflagellate cyst

zonation for North-East Greenland', *Geological Magazine*, this issue.

O'Brien, C. L. *et al.* (2017) 'Cretaceous sea-surface temperature evolution: Constraints from TEX86 and planktonic foraminiferal oxygen isotopes', *Earth-Science Reviews*, pp. 224–247. doi: 10.1016/j.earscirev.2017.07.012.

Ogg, J. G., Hinnov, L. A. and Huang, C. (2012) 'Cretaceous', in *The Geologic Time Scale 2012*, pp. 793–853. doi: 10.1016/B978-0-444-59425-9.00027-5.

Ogg, J. G., Ogg, G. M. and Gradstein, F. M. (2016) '13 - Cretaceous', in Ogg, J. G., Ogg, G. M., and Gradstein, F. M. (eds) *A Concise Geologic Time Scale*. Elsevier, pp. 167–186. doi: https://doi.org/10.1016/B978-0-444-59467-9.00013-3.

Parker, J. R. (1967) 'The Jurassic and Cretaceous Sequence in Spitsbergen', *Geological Magazine*. doi: 10.1017/S0016756800049220.

Pedersen, G. K. and Nøhr-Hansen, H. (2014) 'Sedimentary successions and palynoevent stratigraphy from the non-marine Lower Cretaceous to the marine Upper Cretaceous of the Nuussuaq Basin, West Greenland', *Bulletin of Canadian Petroleum Geology*, 64(4), pp. 261–288. doi: doi.org/10.2113/gscpgbull.62.4.261.

Pestchevitskaya, E. B. (2007) 'Dinocyst biostratigraphy of the Lower Cretaceous in North Siberia', *Stratigraphy and Geological Correlation*, 15(6), pp. 577–609. doi: 10.1134/s0869593807060020.

Pestchevitskaya, E., Lebedeva, N. and Ryabokon, A. (2011) 'Uppermost Jurassic and lowermost Cretaceous dinocyst successions of Siberia, the Subarctic Urals and Russian platform and their interregional correlation', *Geologica Carpathica*, 62(3), pp. 189–202. doi: 10.2478/v10096-011-0016-9.

Piasecki, S. (1979) 'Hauterivian dinoflagellate cysts from Milne Land, East Greenland', *Bulletin of the Geological Society of Denmark*, 28, pp. 31–37.

Piasecki, S., Nøhr-Hansen, H. and Dalhoff, F. (2018) 'Revised stratigraphy of Kap Rigsdagen beds, Wandel Sea Basin, North Greenland', *Newsletters on Stratigraphy*. doi: 10.1127/nos/2018/0444.

Pocock, S. A. J. (1976) 'A Preliminary Dinoflagellate Zonation of the Uppermost Jurassic and Lower Part of the Cretaceous, Canadian Arctic, and Possible Correlation in the Western Canada Basin', *Proceedings of the Annual Meeting. American Association of Stratigraphic Palynologists*. [American Association of Stratigraphic Palynologists, Taylor & Francis, Ltd.], 7, pp. 101–114. doi: 10.2307/3687262.

Polteau, S. *et al.* (2016) 'The Early Cretaceous Barents Sea Sill Complex: Distribution, 40Ar/39Ar geochronology, and implications for carbon gas formation', *Palaeogeography, Palaeoclimatology, Palaeoecology*. Elsevier, 441, pp. 83–95. doi: 10.1016/J.PALAEO.2015.07.007.

Price, G. D. and Passey, B. H. (2013) 'Dynamic polar climates in a greenhouse world: Evidence from clumped isotope thermometry of early cretaceous belemnites', *Geology*, 41(8), pp. 923–926. doi: 10.1130/G34484.1.

Prössl, K. F. (1990) 'Dinoflagellaten der Kreide - Unter-Hauterive bis Ober-Turon - im niedersächsischen Becken. Stratigraphie und Fazies in der Kernbohrung Konrad 101 sowie einiger anderer Bohrungen in Nordwestdeutschland', *Palaeontographica Abteilung B*. Stuttgart, Germany: Schweizerbart Science Publishers, 218(4–6), pp. 93–191.

Rakociński, M. *et al.* (2018) 'Redox conditions, productivity, and volcanic input during deposition of uppermost Jurassic and Lower Cretaceous organic-rich siltstones in Spitsbergen, Norway', *Cretaceous Research*, 89, pp. 126–147. doi: 10.1016/j.cretres.2018.02.014.

Riding, J. B. (1999) *Jurassic and lowermost Cretaceous dinoflagellate cyst biostratigraphy of the Russian Platform and Northern Siberia, Russia*. AASP contr. American Association of Stratigraphic Palynologists Foundation (1999).

Rogers, J. J. W. and Santosh, M. (2004) 'Continents and Supercontinents', *Gondwana Research*. doi: 10.1016/S1342-937X(05)70827-3.

Scotese, C. (2014) *Atlas of Early Cretaceous Paleogeographic Maps, PALEOMAP Atlas for ArcGIS, volume 2, The Cretaceous, Maps 23 - 31, Mollweide Projection, PALEOMAP Project, Evanston, IL.* doi: 10.13140/2.1.4099.4560.

Senger, K. *et al.* (2014) 'Late Mesozoic magmatism in Svalbard: A review', *Earth-Science Reviews*, 139, pp. 123–144. doi: 10.1016/j.earscirev.2014.09.002.

Śliwińska, K. K. (2019) 'Early Oligocene dinocysts as a tool for palaeoenvironment reconstruction and stratigraphical framework – a case study from a North Sea well', *J. Micropalaeontol.* Copernicus Publications, 38(2), pp. 143–176. doi: 10.5194/jm-38-143-2019.

Smelror, M. (1986) 'Jurassic and Lower Cretaceous palynomorph assemblages from Cape Flora, Franz Josef Land, Arctic USSR.', *Norsk Geologisk Tidsskrift*.

Smelror, M. *et al.* (1998) 'The Klippfisk Formation - a new lithostratigraphic unit of Lower Cretaceous platform carbonates on the Western Barents Shelf', *Polar Research*, 17(2),

pp. 181–202. doi: 10.1111/j.1751-8369.1998.tb00271.x.

Smelror, M. *et al.* (2018) 'Late Triassic to Early Cretaceous palynostratigraphy of Kong Karls Land, Svalbard, Arctic Norway, with correlations to Franz Josef Land, Arctic Russia', *Norwegian Journal of Geology*, 98(04), pp. 1–31. doi: https://dx.doi.org/10.17850/njg98-4-04.

Smelror, M. and Dypvik, H. (2005a) 'Marine microplankton biostratigraphy of the Volgian-Ryazanian boundary strata, western Barents Shelf', *NGU Bulletin*, 443, pp. 61–69.

Smelror, M. and Dypvik, H. (2005b) 'The Sweet Aftermath: Environmental Changes and Biotic Restoration Following the Marine Mjølnir Impact (Volgian-Ryazanian Boundary, Barents Shelf)', in *Biological Processes Associated with Impact Events*, pp. 143–178. doi: 10.1007/3-540-25736-5_7.

Smelror, M. and Larssen, G. B. (2016) 'Are there upper cretaceous sedimentary rocks preserved on sørkapp land, Svalbard?', *Norsk Geologisk Tidsskrift*, 96(2), pp. 1–12. doi: 10.17850/njg96-2-05.

Thusu, B. (1978) 'Aptian to Toarcian dinoflagellate cysts from Arctic Norway', in Thusu, Bindra (ed.) *Distribution of biostratigraphically diagnostic dinoflagellate cysts and miospore from Northwest European continental shelf and adjacent areas*. Continental Shelf Institute, pp. 61–95.

Torsvik, T. H. *et al.* (2002) 'Global reconstructions and North Atlantic paleogeography 440 Ma to Recent', *Batlas - Mid Norway plate reconstruction atlas with global and Atlantic perspectives*, pp. 18–39.

Trabucho Alexandre, J. *et al.* (2010) 'The mid-Cretaceous North Atlantic nutrient trap: Black shales and OAEs', *Paleoceanography*. doi: 10.1029/2010PA001925.

Vickers, M. L. *et al.* (2016) 'Stratigraphic and geochemical expression of Barremian-Aptian global climate change in Arctic Svalbard', *Geosphere*, 12(5), pp. 1594–1605. doi: 10.1130/GES01344.1.

Vozzhennikova, T. F. (1967) *Iskopaemye peridinei Yurskikh, Melovykh i Paleogenovykh otlozheniy SSSR*. Moscow, U.S.S.R.: Izdatelstvo Nauka.

Wierzbowski, A. *et al.* (2011) 'Ammonites from hydrocarbon seep carbonate bodies from the uppermost Jurassic – lowermost Cretaceous of Spitsbergen and their biostratigraphical importance', *Neues Jahrbuch für Geologie und Paläontologie - Abhandlungen*, 262(3), pp. 267–288. doi: 10.1127/0077-7749/2011/0198.

Williams, G., Fensome, R. and MacRae, R. (2017) 'The Lentins and Williams Index of Fossil Dinoflagellates 2017 Edition', *AASP Contributions Series*, 48(48), pp. 1–1097.

Zakharov, V. A. (1987) 'The bivalve Buchia and the Jurassic-Cretaceous boundary in the boreal province', *Cretaceous Research*. doi: 10.1016/0195-6671(87)90018-8.

Table 1. List of palynomorphs recorded in this study including a reference for photographs (Figs. 6-9) and range charts (Figs S1-S6)

Palynomorph name in alphabetical order according to genus then species	Photo	Fig. S1	Fig. S2	Fig. S3	Fig. S4	Fig. S5	Fig S6
Apteodinium spongiosum	9b-e		35		5		21
Apteodinium spp.				1			28
Athigmatocysta glabra							33
Atopodinium haromense	9f	37	58	34			
Bourkidinium granulatum			33				
Bourkidinium spp.				32			
Canningia reticulata				23			
Cassiculosphaeridia magna							10
Chlamydophorella nyei				27	18		
Chlamydophorella spp.				2			
Circulodinium aff. *attadalicum* sensu Nøhr-Hansen 1993				28		33	
Circulodinium distinctum	6g-j	42	15	35	8	19	25
Circulodinium sp. 1			32				
Circulodinium spp.		8	36	12	19	26	31
Cleistosphaeridium spp.			44				37
Cribroperidinium sp. 1			6	31			
Cribroperidinium spp.		9	12		6	14	4
Cyclonephelium cuculliforme sensu Århus 1990	8l		10				
Dinocyst sp. A	9d						
Dingodinium cerviculum	6n	5	37	7	14	9	16
Discorsia nannus	6m	27	34				47
Dissiliodinium acmeum	6k		8				
Downiesphaeridium? aciculare		45	64		23	27	54
Endoscrinium hauterivianum	6o,p	22	56	39	33	13,38	36
Endoscrinium sp. 1	6l	1	51		1	3	29
Endoscrinium spp.				38			
? Escharisphaeridia rudis	8b		27				32
Florentinia spp.				3			
Gardodinium trabeculosum		43	65				
Gochteodinia judilentiniae			25				
Gochteodinia villosa subsp. *multifurcata*	7a,c		28		2		12
Gochteodinia villosa	7b		29			39	11
Gonyaulacysta sp. 1			41				
Gonyaulacysta spp.		25	16	30			14
Heslertonia heslertonensis		30	31				
Hystrichodinium voigtii		35	22				46
Hystrichosphaeridium arborispinum							49
Isthmocystis distincta	7i		23				

Kiokansium unituberculatum	7k	19	38		35		42
Kleithriasphaeridium eoinodes	7j		55				
Lagenorhytis delicatula							22
Leptodinium spp.		21					
Meiourogonyaulax stoveri	7l	33	43				35
Muderongia asymmetrica							55
Muderongia australis	7e	40	62	40	30	15	43
Muderongia extensiva	7h	39					
Muderongia pariata						36	52
Muderongia simplex	7f		46				44
Muderongia simplex subsp. *Microperforata* sensu Nøhr-Hansen 1993							56
Muderongia spp.		10	50	24	9	17	45
Muderongia tetracantha		36	61	10	22		40
Muderongia tetracantha/extensiva	7g	31	59		28		41
Nelchinopsis kostromiensis	7m,n	6	39	4,41	27	10	18
Nyktericysta? aff. *pannosa*	7o,p	41			20		
Nyktericysta vitrea						34	
Nyktericysta spp.							57
Odontochitina nuda	8e			36		30	
Odontochitina spp.				26			
Oligosphaeridium albertense				22			
Oligosphaeridium abaculum	8f	11	53		7	22	34
Oligosphaeridium asterigerum	8i	12	24	13	12	1	26
Oligosphaeridium complex	8h	13	17	18	15	4	19
Oligosphaeridium complex var. 1					3	2	
Oligosphaeridium poculum	8a	2	13	14	16	18	27
Oligosphaeridium aff. *pulcherrimum*				9			
Oligosphaeridium spp.		14	18	17	4	23	24
Oligosphaeridium with broken processes		7	19	19	13	7	20
Other dinocysts		15	20	15	21	20	5
Palaecysta palmula	8k		3				
Palaeoperidinium cretaceum						37	
Palynomorph A			57				8
Palynomorph B				11			
Paragonyaulacysta capillosa			4				
Paragonyaulacysta spp.			42	33	24	6	
Pareodinia spp.		23	14	25	34	21	38
Phoberocysta neocomica	8c	17	47		31		
Prolixosphaeridiopsis spissa (acritarch)			26				
Pseudoceratium anaphrissum	8m-o	46		16		31	
Pseudoceratium pelliferum	8j	29	60	5	10	32	39
Pseudoceratium cf. *retusum* sensu Nøhr-Hansen 1993						35	
Pseudoceratium spp.							51
Rhynchodiniopsis aptiana	8d,g	16	48		36		48

Rhynchodiniopsis spp.					25		
Sepispinula? huguoniotii			52				
Scriniodinium campanula				37		24	
Sirmiodinium grossii	9e,f	24	2	20	17	8	3
Spiniferites sp. 1	9d		54		29		30
Spiniferites spp.	9h		49	6			
Stanfordella fastigiata	9a	20	9	26	32	5	15
Stanfordella ordocava	9b,c		30		38	11	13
Stiphrosphaeridium anthophorum			63				
Subtilisphaera perlucida	9g			8		28	
Tanyosphaeridium boletus		34	45			29	53
Tanyosphaeridium salpinx		28	40		37	25	23
Tanyosphaeridium spp.					26		17
Tubotuberella apatela	9i-k	47	1,66	42	39	40	1
Tubotuberella uncinata		32					
Tubotuberella spp.	9l	38	11	43	11		2,58
Wallodinium luna	9m						9
Wrevittia helicoidea		44	5				7
cf. *Wrevittia perforobtusa*	9n-p	26	7			12	50
unidentifiable dinocysts		4	21	21		16	6

1362

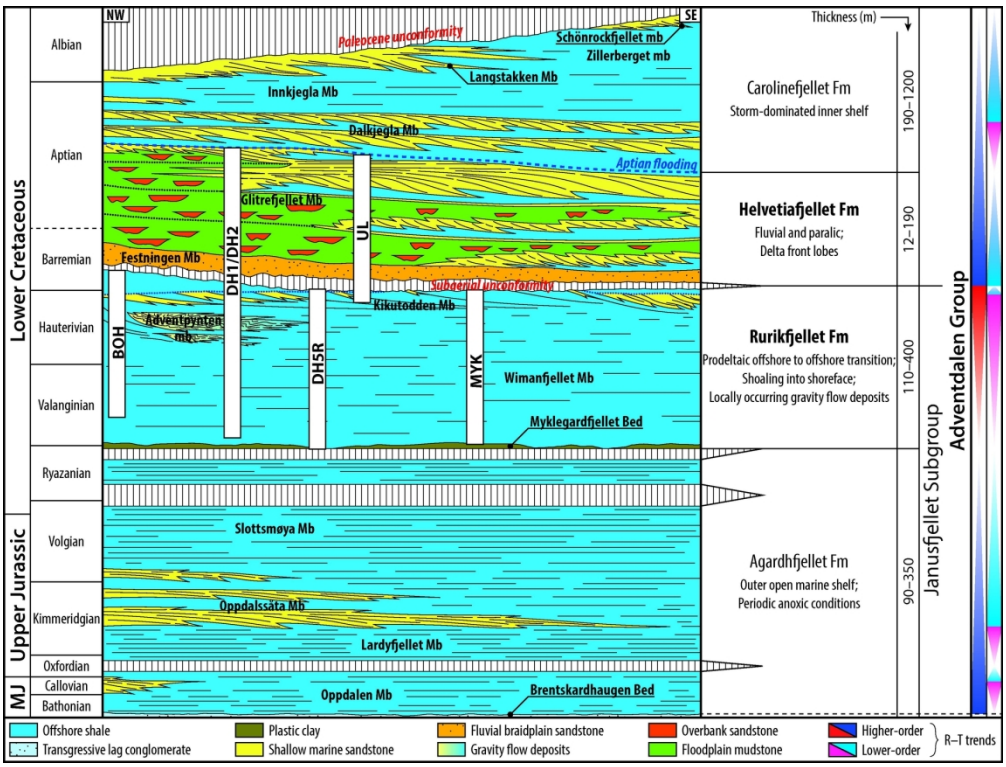

Figure 1. Stratigraphic cross-section showing the regional development of the Upper Jurassic to Lower Cretaceous Adventdalen Group on Spitsbergen. Modified after Alsen et al. (this issue). White bars show the time span for each of the studied sites: three onshore cores DH1, DH2, DH5R, and three outcrop sections: Bohemanflya (BOH), Ullaberget (UL), and Myklegardfjellet (MYK). The figure is available in colour on the web version of this paper.

169x128mm (300 x 300 DPI)

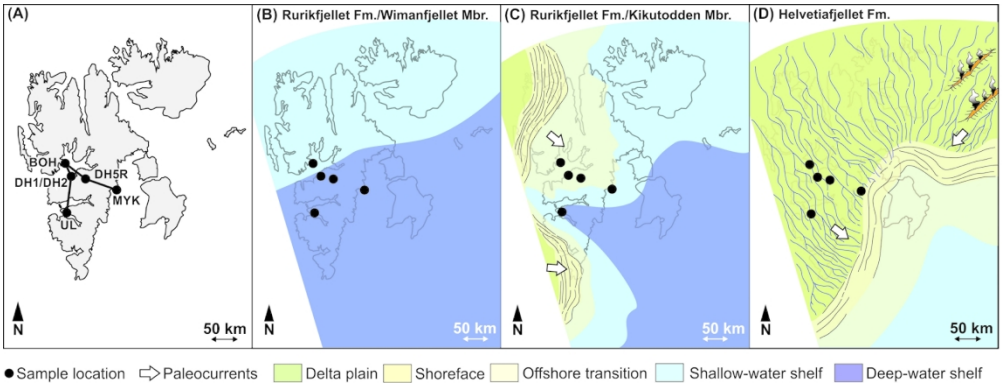

Figure 2. (A). Black dots mark the positions of the studied sites: Bo – Bohemanflya, Ul – Ullaberget, My – Myklegardfjellet outcrop sections. Paleogeography of Spitsbergen from the Valanginian to early Aptian (after Grundvåg & Olaussen, 2017; Grundvåg et al., 2017) (B) Palaeogeography during the deposition of the Wimanfjellet Member; (C) Palaeogeography during the deposition of the Kikutodden Member; (D) Paleogeography during the earliest Barremian - deposition of the Festningen Member.

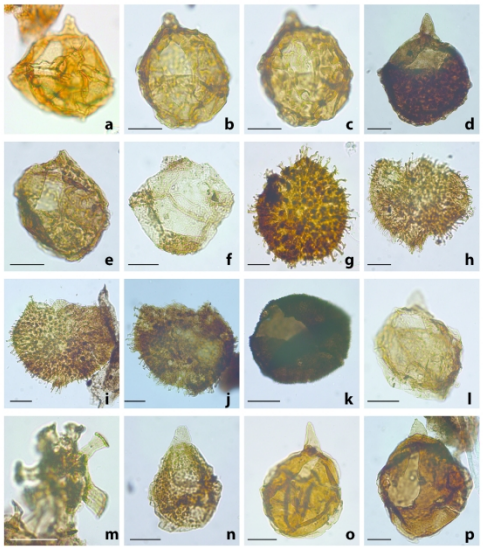

Figure 3. Photographs of the most characteristic dinoflagellate cysts observed in the Rurikfjellet and Helvetiafjellet formations in the present study. Scale bars on all photographs represent 20 µm. The figure is available in colour on the web version of this paper. MC – microscope coordinates with the A-point of 0.4×90.3 (XM1 × YM1). For details, see Śliwińska (2019).(a) a dinocyst, Bohemanflya outcrop section, level 99.29 m, sample 26291-7, MC 102 x 42.2(b) Apteodinium spongiosum, high focus, (c) low focus, Bohemanflya outcrop section, level 25.00 m, sample 28450-9, MC 25 x 108.7(d) Apteodinium spongiosum very dark, Myklegardfjellet outcrop section, level 30.00 m, sample 27007-6, MC 32 x 109.1(e) Apteodinium spongiosum, Myklegardfjellet outcrop section, level 120.00 m, sample 27013-9; MC 51.4 x 105.5(f) Atopodinium haromense; Myklegardfjellet outcrop section, level 120.00 m, sample 27013-9; MC 42.7 x 102.3 (g) Circulodinium distinctum, Myklegardfjellet outcrop section, level 105.00 m, sample 27012-6; MC 29.3 x 91.6(h) Circulodinium distinctum, Myklegardfjellet outcrop section, level 120.00 m, sample 27013-9; MC 21 x 104.5 (i) Circulodinium distinctum, Myklegardfjellet outcrop section, level 120.00 m, sample 27013-9; MC 17.5 x 105.5 (j) Circulodinium distinctum, Bohemanflya outcrop section, level 28.00 m, sample 28449-8; MC 44.7 x 96.7(k) Dissiliodinium acmeum, Myklegardfjellet outcrop section, level 7.00 m, sample 27005-4; MC 37.2 x 99.4(l) Endoscrinium sp.1 Bohemanflya outcrop section, level 25.00 m, sample 28450-9; MC 25.5 x 110(m) Discorsia nannus, Myklegardfjellet outcrop section, level 120.00 m, sample 27013-9; MC 49 x 103.3(n) Dingodinium cerviculum, Myklegardfjellet outcrop section, level 75.00 m, sample 27010-4; MC 47 x 108.5(o) Endoscrinium hauterivianum, Bohemanflya outcrop section, level 36.00 m, sample 28448-7, MC 33.8 x 102.2(p) Endoscrinium hauterivianum, Myklegardfjellet outcrop section, level 120.00 m, sample 27013-9; MC 42 x 102.4

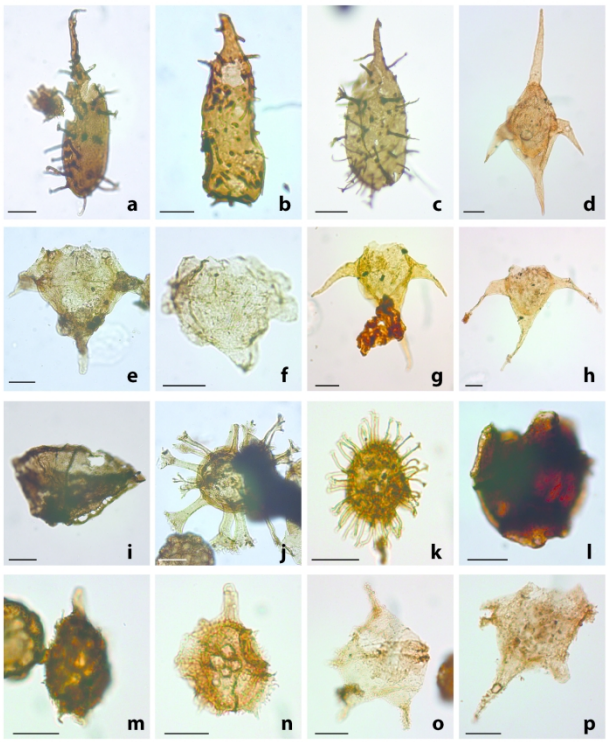

Figure 4. Photographs of the most characteristic dinoflagellate cysts observed in the Rurikfjellet and Helvetiafjellet formations in the present study. Scale bars on all photographs represent 20 µm. The figure in colour is available on the web version of this paper. MC – microscope coordinates with the A-point of 0.4×90.3 (XM1 × YM1). For details, see Śliwińska (2019).
(a) Gochteodinia villosa subsp. multifurcata, Myklegardfjellet outcrop section, level 15.00 m, sample 27006-5, MC 36.3 x 114
(b) Gochteodinia villosa, DH5R core, depth 350.00 m, sample 26197-6; MC 22.5 x 96.2
(c) Gochteodinia villosa subsp. multifurcata, Myklegardfjellet outcrop section, level 15.00 m, sample 27006-5; MC 36 x 107
(d) Muderongia tetracanta, Bohemanflya outcrop section, level 127.50 m, sample 26290-8, MC 44 x 110.6
(e) Muderongia australis, Myklegardfjellet outcrop section, level 120.00 m, sample 27013-9; MC 31.4 x 108.5
(f) Muderongia simplex, Myklegardfjellet outcrop section, level 105.00 m, sample 27012-6; MC 33 x 105.8
(g) a transitional form between Muderongia tetracanta and Muderongia extensiva, Bohemanflya outcrop section, level 46.00 m, sample 26293-5, MC 24.5 x 111
(h) Muderongia extensiva, Bohemanflya outcrop section, level 46.00 m, sample 26293-7; MC 18.5 x 108.4
(i) Isthmocystis distincta, Myklegardfjellet outcrop section, level 7.00 m, sample 27005-4; MC 28 x 102.3
(j) Kleithriasphaeridium eoinodes, Myklegardfjellet outcrop section, level 90.00 m, sample 27011-8; MC 25.2 x 103
(k) Kiokansium unituberculatum, Bohemanflya outcrop section, level 127.50, sample 26290-6; MC 31x107.3
(l) Meiourogonyaulax stoveri, DH5R core, depth 258.00 m, sample 26194-5; MC 24 x 107.8
(m) poorly preserved Nelchinopsis kostromiensis, Bohemanflya outcrop section, level 99.29 m, sample

26291-7; MC 52.4 x 109
(n) Nelchinopsis kostromiensis, Bohemanflya outcrop section, level 55.25 m, sample 26292-7; MC 51.5 x 95.5
(o) Nyktericysta? pannosa, Bohemanflya outcrop section, level 99.29 m, sample 26291-7; MC 43 x 102.7
(p) Nyktericysta? pannosa, Bohemanflya outcrop section, level 127.50 m, sample 26290-8; MC 50.2 x 100

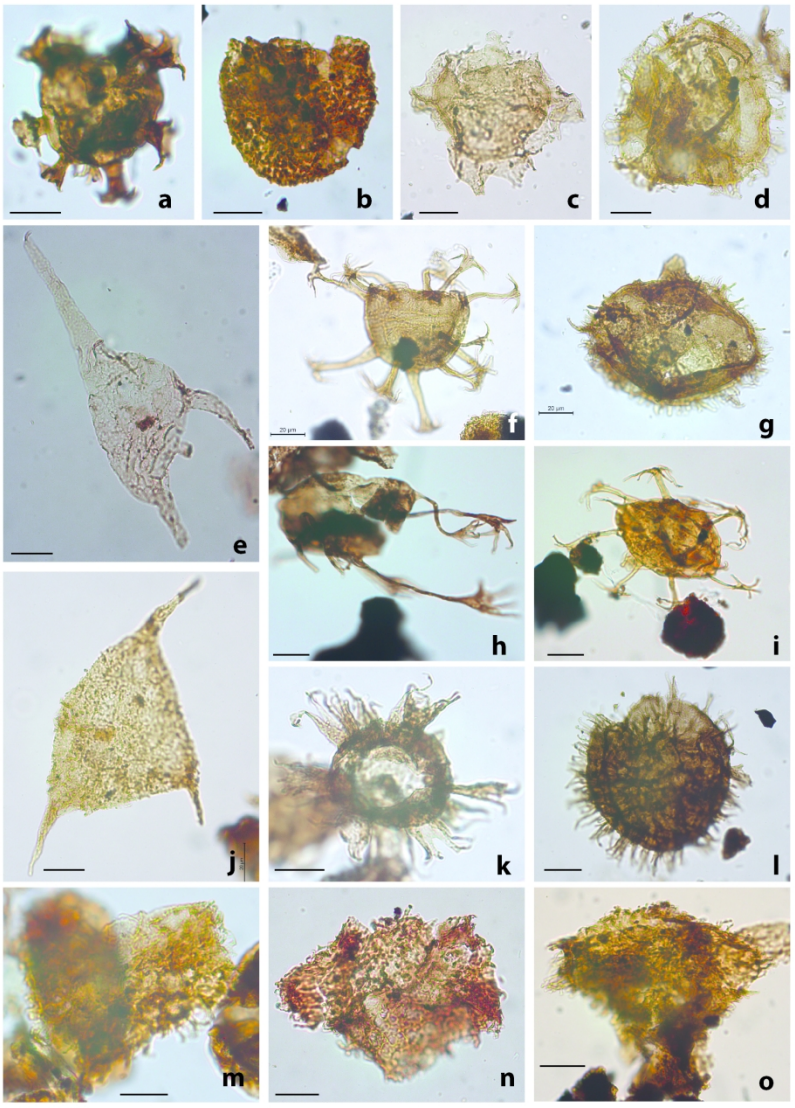

Figure 5. Photographs of the most characteristic dinoflagellate cysts observed in the Rurikfjellet and Helvetiafjellet formations in the present study. Scale bars on all photographs represent 20 µm. The figure in colour is available on the web version of this paper. MC – microscope coordinates with the A-point of 0.4×90.3 (XM1 × YM1). For details, see Śliwińska (2019).
(a) Oligosphaeridium poculum, DH5R core, depth 320.00 m, sample 26196-7; MC 58.2 x 97.1
(b) questionable Escharisphaeridia rudis, DH5R core, depth 288.00 m, sample 26195-7; MC 36.7 x 112.5
(c) Phoberocysta neocomica, Myklegardfjellet outcrop section, level 90.00 m, sample 27009-6; MC 24.3 x 113.8
(d) Rhynchodiniopsis aptiana, Bohemanflya outcrop section, level 5.00 m, sample 28453-7, MC 31.7 x 101
(e) Odontochitina nuda, DH2 core, depth 141.80 m, sample 26510-9; MC 42 x 105.2
(f) Oligosphaeridium abaculum, Myklegardfjellet outcrop section, level 75.00 m, sample 27010-5; MC 48.5 x 105.5
(g) Rhynchodiniopsis aptiana, Myklegardfjellet outcrop section, level 105.00 m, sample 27012-6; MC 20.3 x 107.5

(h) Oligosphaeridium complex with "palm-like" terminations of processes, DH1, depth 258.90 m, sample 26285-7; MC 32.8 x 97.1
(i) Oligosphaeridium asterigerum, Bohemanflya outcrop section, level 99.29 m, sample 26291-7, MC 44.7 x 94.3
(j) Pseudoceratium pelliferum, Bohemanflya outcrop section, level 36.00 m, sample 28448-7, MC 37 x 106.5
(k) Palaecysta palmula, Myklegardfjellet outcrop section, level 0.05 m, sample 27004-8, MC 53 x 107.5
(l) Cyclonephelium cuculliforme sensu Århus 1990, Myklegardfjellet outcrop section, level 15.00, sample 27006-3; MC 30.2 x 101
(m) questionable Pseudoceratium anaphrissum Bohemanflya outcrop section, level 132.63 m, sample 26289-8; MC 37.8 x 95.5. Shown also in Figure 15.P in Grundvåg et al., (2019).
(n) Pseudoceratium anaphrissum, Ullaberget outcrop section, level 104.00m, sample 28482-7; MC 40.6 x 111.8
(o) questionable, poorly preserved Pseudoceratium anaphrissum, DH2 core, depth 149.50 m, sample 26511-11; MC 34.5 x 110.5. Shown also in Figure 15.H in Grundvåg et al., (2019).

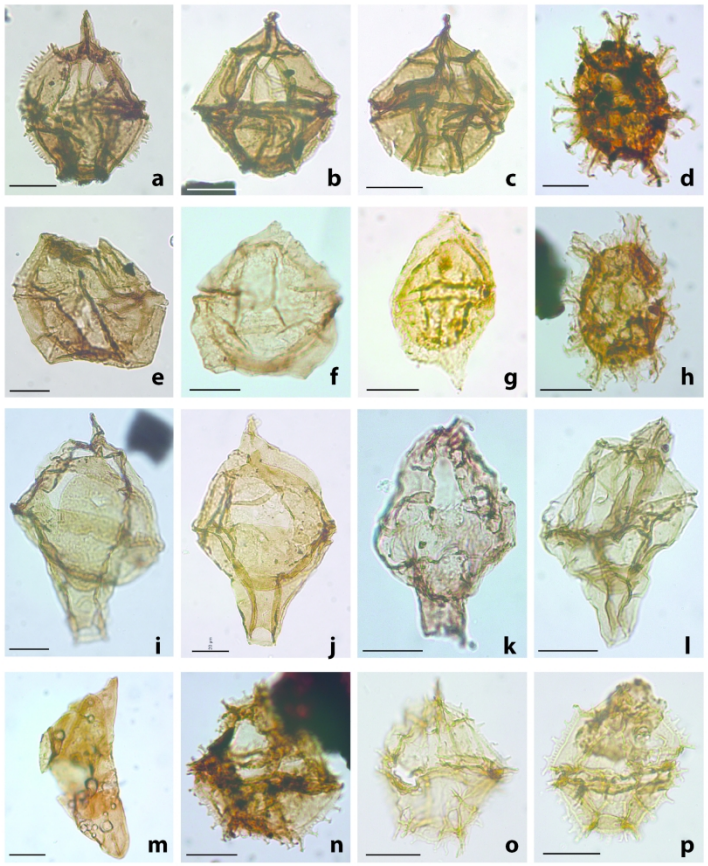

Figure 6. Photographs of the most characteristic dinoflagellate cysts observed in the Rurikfjellet and Helvetiafjellet formations in the present study. Scale bars on all photographs represent 20 µm. The figure in colour is available on the web version of this paper. MC – microscope coordinates with the A-point of 0.4×90.3 (XM1 × YM1). For details, see Śliwińska (2019).
(a) Stanfordella fastigiata, Myklegardfjellet outcrop section, level 30.00 m, sample 27007-6; MC 50.4 x 103.5
(b) Stanfordella ordocava, Myklegardfjellet outcrop section, level 15.00 m, sample 27006-5; MC 31.6 x 111
(c) Stanfordella ordocava, DH5R core, depth 380.00 m, sample 26198-6; MC 55.5 x 102.4
(d) Spiniferites sp. 1, DH5R core, depth 194.00 m, sample 26192-7; MC 36.9 x 102
(e) Sirmiodinium grossii, Myklegardfjellet outcrop section, level 30.00 m, sample 27007-6; MC 30.3 x 104.2
(f) Sirmiodinium grossii, DH1, depth 258.90 m, sample 26285-7; MC 29.4 x 109
(g) Subtilisphaera perlucida, DH2 core, depth 186.55 m, sample 26513-9; MC 36.7 x 92.6. Shown also in Figure 15.G in Grundvåg et al., (2019).
(h) Spiniferites? DH5R core, depth 194.00 m, sample 26192-7; MC 50.8 x 101.2
(i) Tubotuberella apatela, Myklegardfjellet outcrop section, level 30.00 m, sample 27007-6; MC 30.6 x 105
(j) Tubotuberella apatela, Myklegardfjellet outcrop section, level 0.05 m, sample 27004-8; MC 34.5 x 109.4
(k) Tubotuberella apatela, DH2 core, depth 232.00 m, sample 26516-9; MC 19.4 x 93.3
(l) Tubotuberella sp. DH5R core, depth 380.0 m, sample 26198-6; MC 48 x 98.7

(m) Wallodinium luna, DH5R core, depth 350.0 m, sample 26197-6; MC 36.5 x 102.4
(n) Wrevittia perforobtusa, DH5R core, depth 194.00 m, sample 26192-7; MC 29.9 x 102.6
(o) Wrevittia perforobtusa, Bohemanflya outcrop section, level 55.25 m, sample 26292-8, MC 50.3 x 101.7
(p) Wrevittia perforobtusa, Bohemanflya outcrop section, level 36 m, sample 28448-7, MC 40.5 x 98.6

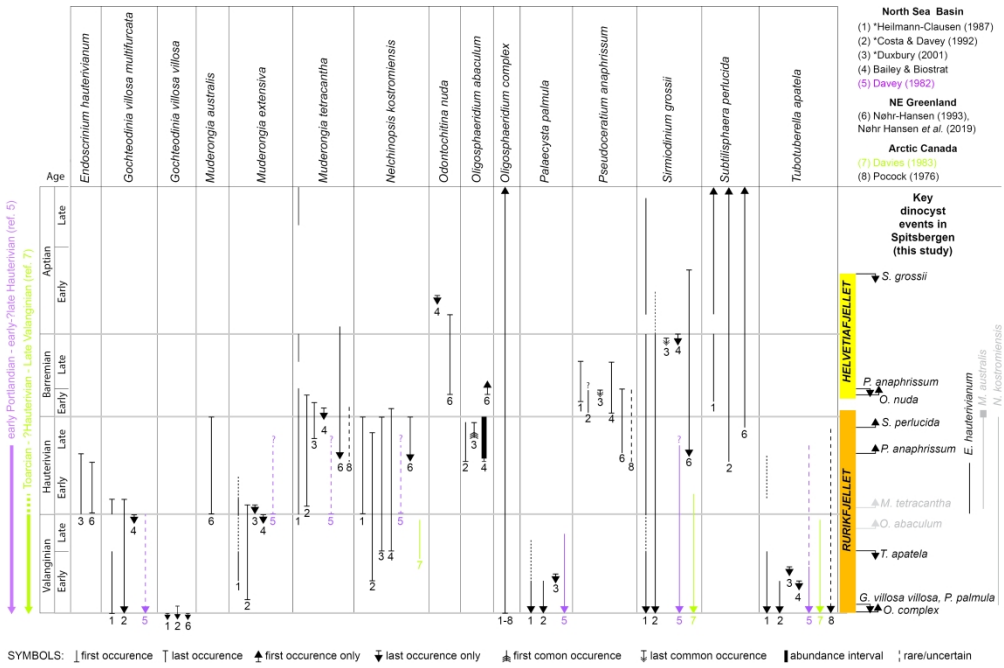

Figure 7. The stratigraphic ranges and/or first and last occurrences of the age diagnostic dinoflagellate cysts (dinocysts) from the Boreal and European Boreal Realm, and the key events recognised in this study (to the right). Key dinocyst events in Spitsbergen: primary markers (black), secondary markers (grey).
The figure shows a compilation of the most characteristic dinocysts from the Rurikfjellet and Helvetiafjellet formations discussed in the present study. Heilmann-Clausen (1987), Costa & Davey (1992), and Duxbury (2001) plotted the dinocysts ranges against the ammonite zonation (marked with asterix). All these authors considered the Simbirskites variabilis ammonite zone as earliest Barremian, whilst today it is considered to be Hauterivian (Ogg, Ogg & Gradstein, 2016). Nøhr-Hansen, Piasecki & Alsen (this issue) updated the zonation proposed previously by Nøhr-Hansen (1993), and provided ages in GTS2016. Note that the study by Davey (1982) does not cover sediments younger than early-?late Hauterivian, while the study by Davies (1983) does not cover sediments younger than late Valanginian.

415x273mm (300 x 300 DPI)

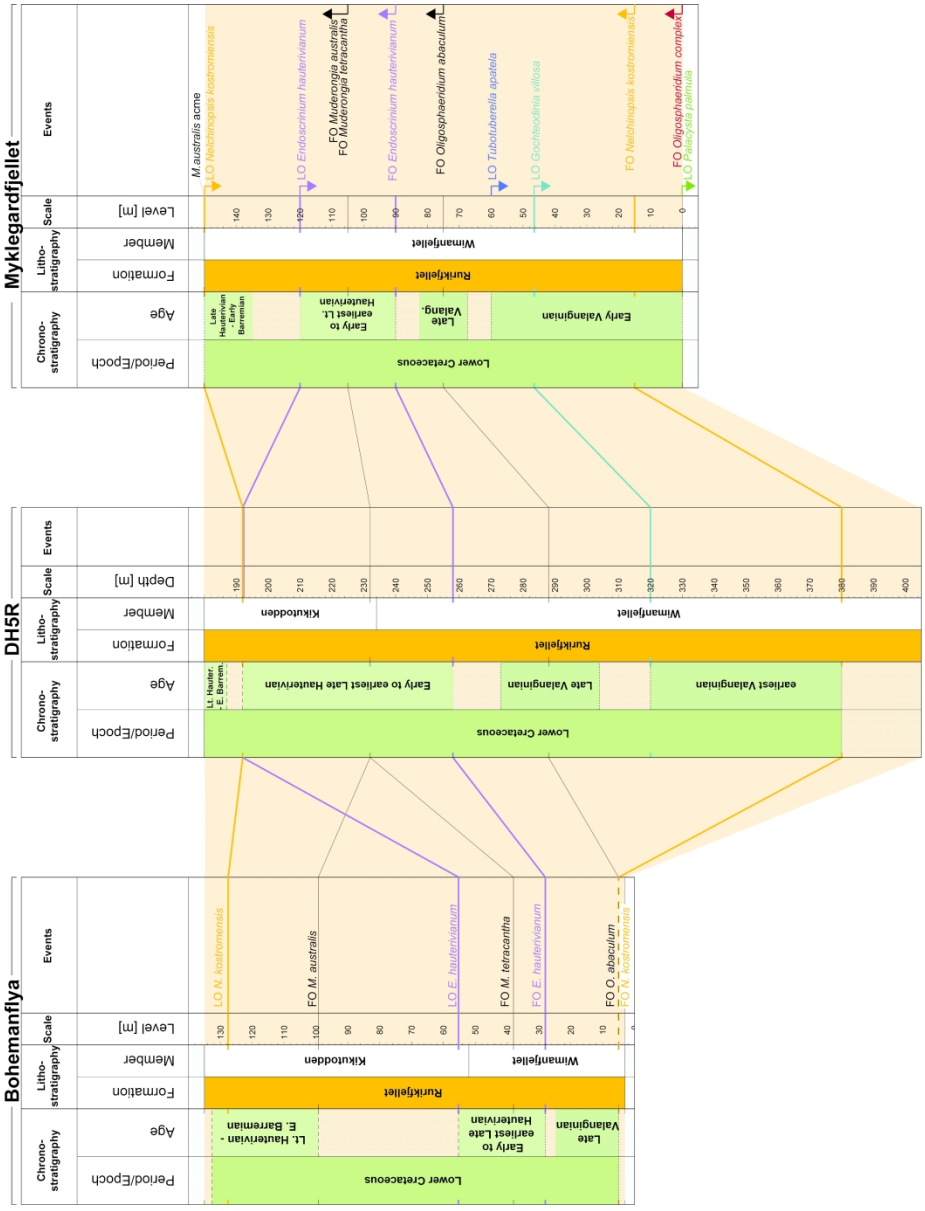

Figure 8. The spatial distribution of the age diagnostic (colour code) and secondary dinocyst events (black) within the Rurikfjellet Formation. The correlation between the Bohemanflya, the DH5R core, and the Myklegardfjellet outcrop section, i.e. from NW to SE.

288x376mm (300 x 300 DPI)

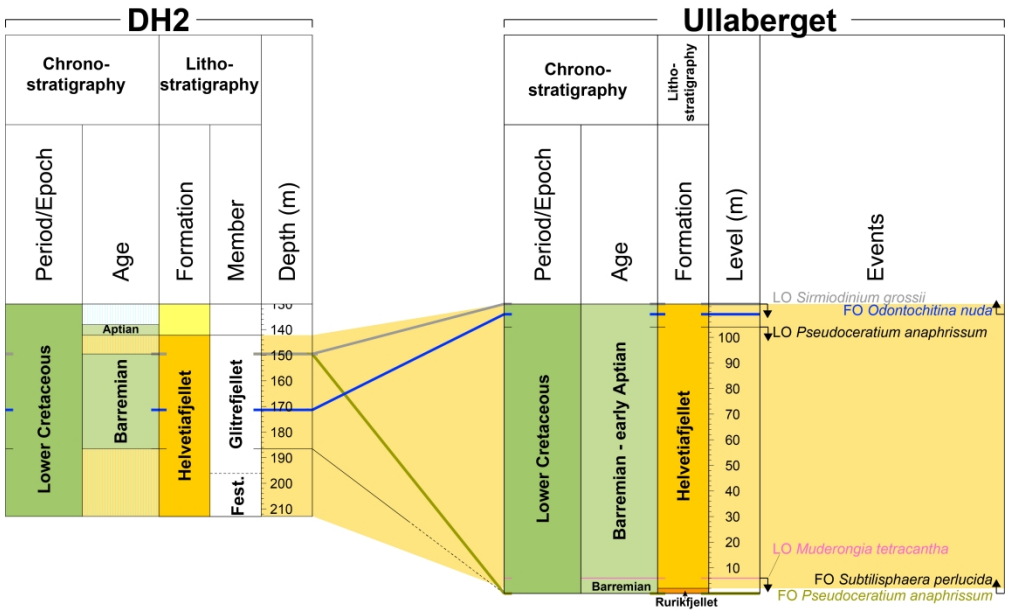

Figure 9. The spatial distribution of the age diagnostic dinocyst events within the Helvetiafjellet Formation. The correlation between the Ullaberget outcrop section and the DH2 core.

390x236mm (300 x 300 DPI)

Geological Magazine

Dinocyst stratigraphy of the Valanginian–Aptian Rurikfjellet and Helvetiafjellet formations on Spitsbergen, Arctic Norway

Kasia K. Śliwińska, Mads E. Jelby, Sten-Andreas Grundvåg, Henrik Nøhr-Hansen, Peter Alsen, and Snorre Olaussen

Supplementary material

Figure S1: Bohemanflya

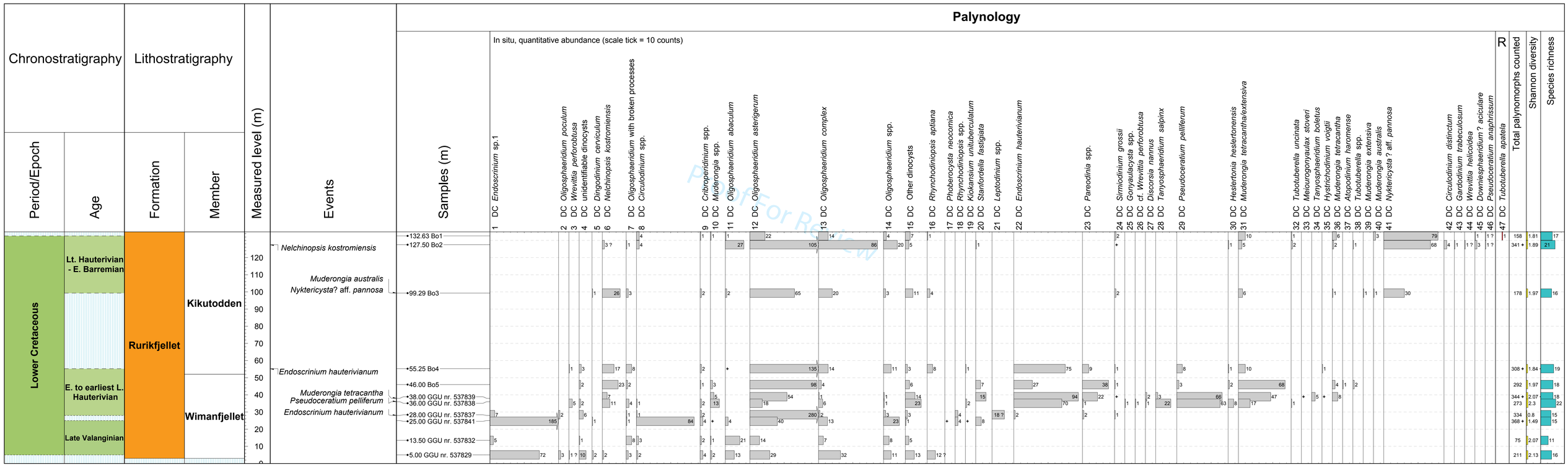

Figure S1. Distribution of dinocysts in the Bohemanflya outcrop section. This file contains range charts with the quantitative data of the palynomorphs recognised in this study.
The palynomorphs are arranged after the first occurrence (FO), R – reworked, DC – dinocyst, AC – acritarch, MP – palynomorph, , "+" – present outside counting, "?" – questionable

Geological Magazine

Dinocyst stratigraphy of the Valanginian–Aptian Rurikfjellet and Helvetiafjellet formations on Spitsbergen, Arctic Norway

Kasia K. Śliwińska, Mads E. Jelby, Sten-Andreas Grundvåg, Henrik Nøhr-Hansen, Peter Alsen, and Snorre Olaussen

Supplementary material

Figure S2: Myklegardfjellet

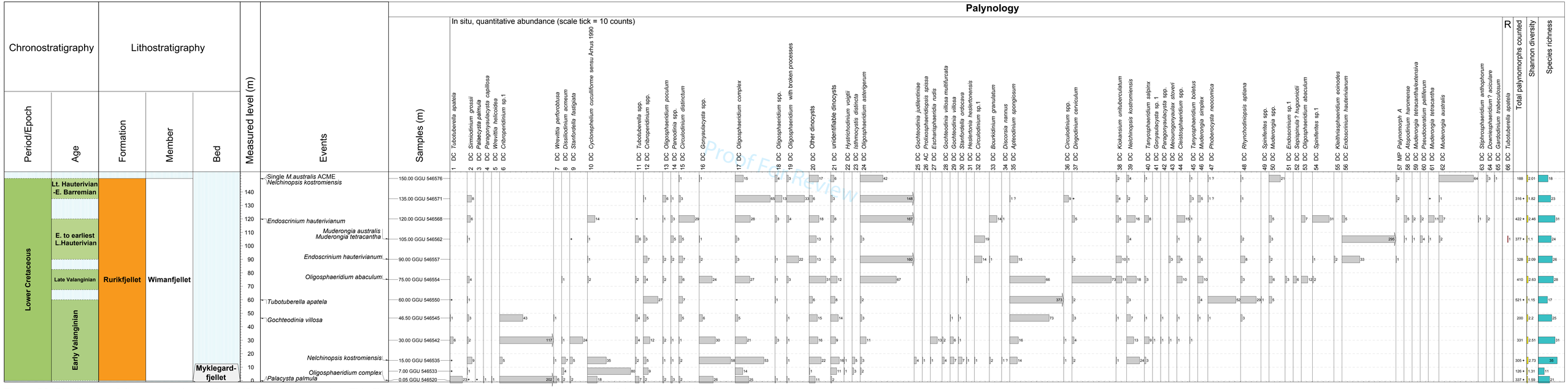

Figure S2. Distribution of dinocysts in the Myklegardfjellet outcrop section. This file contains range charts with the quantitative data of the palynomorphs recognised in this study.
The palynomorphs are arranged after the first occurrence (FO), R – reworked, DC – dinocyst, AC – acritarch, MP – palynomorph, , "+" – present outside counting, "?" – questionable

Geological Magazine

Dinocyst stratigraphy of the Valanginian–Aptian Rurikfjellet and Helvetiafjellet formations on Spitsbergen, Arctic Norway

Kasia K. Śliwińska, Mads E. Jelby, Sten-Andreas Grundvåg, Henrik Nøhr-Hansen, Peter Alsen, and Snorre Olaussen

Supplementary material

Figure S3: Ullaberget

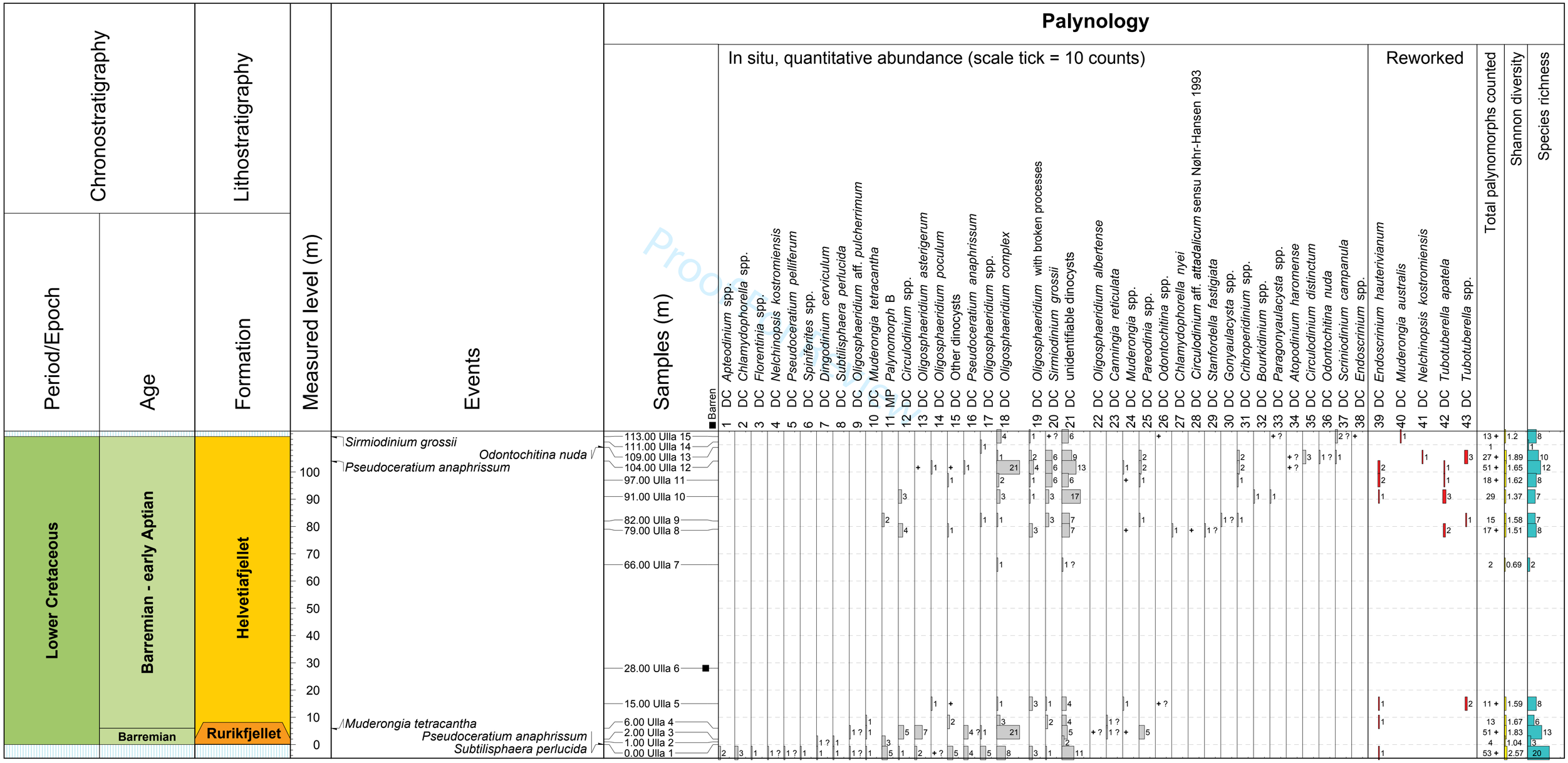

Figure S3. Distribution of dinocysts in the Ullaberget outcrop section. This file contains range charts with the quantitative data of the palynomorphs recognised in this study. The palynomorphs are arranged after the first occurrence (FO), R – reworked, DC – dinocyst, AC – acritarch, MP – palynomorph, , “+” – present outside counting, “?” – questionable

Geological Magazine

Dinocyst stratigraphy of the Valanginian–Aptian Rurikfjellet and Helvetiafjellet formations on Spitsbergen, Arctic Norway

Kasia K. Śliwińska, Mads E. Jelby, Sten-Andreas Grundvåg, Henrik Nøhr-Hansen, Peter Alsen, and Snorre Olaussen

Supplementary material

Figure S4: DH1

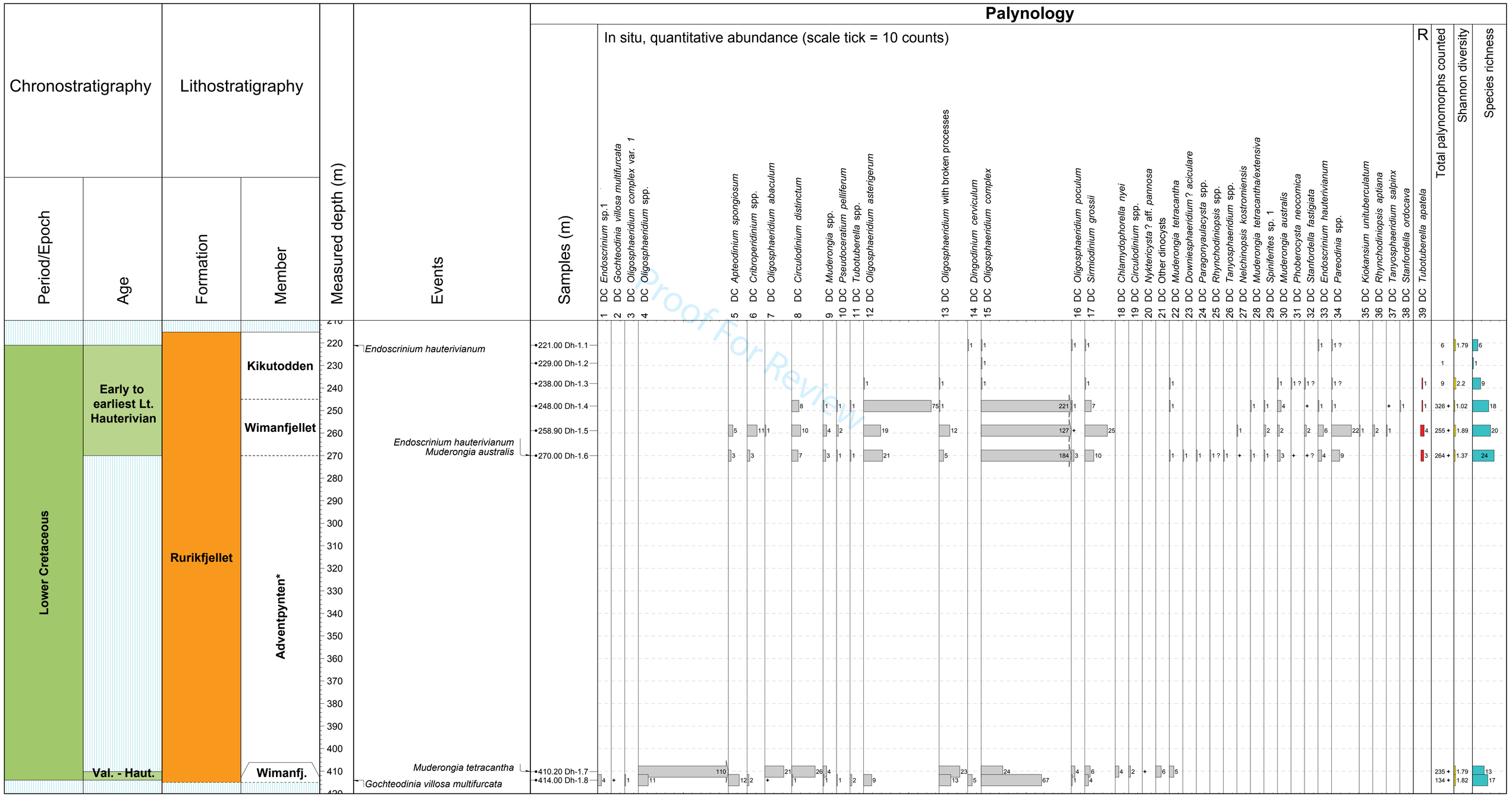

Figure S4. Distribution of dinocysts in the DH1 well. This file contains range charts with the quantitative data of the palynomorphs recognised in this study.
The palynomorphs are arranged after the first occurrence (FO), R – reworked, DC – dinocyst, AC – acritarch, MP – palynomorph, “+” – present outside counting, “?” – questionable

Geological Magazine

Dinocyst stratigraphy of the Valanginian–Aptian Rurikfjellet and Helvetiafjellet formations on Spitsbergen, Arctic Norway

Kasia K. Śliwińska, Mads E. Jelby, Sten-Andreas Grundvåg, Henrik Nøhr-Hansen, Peter Alsen, and Snorre Olaussen

Supplementary material

Figure S5: DH2

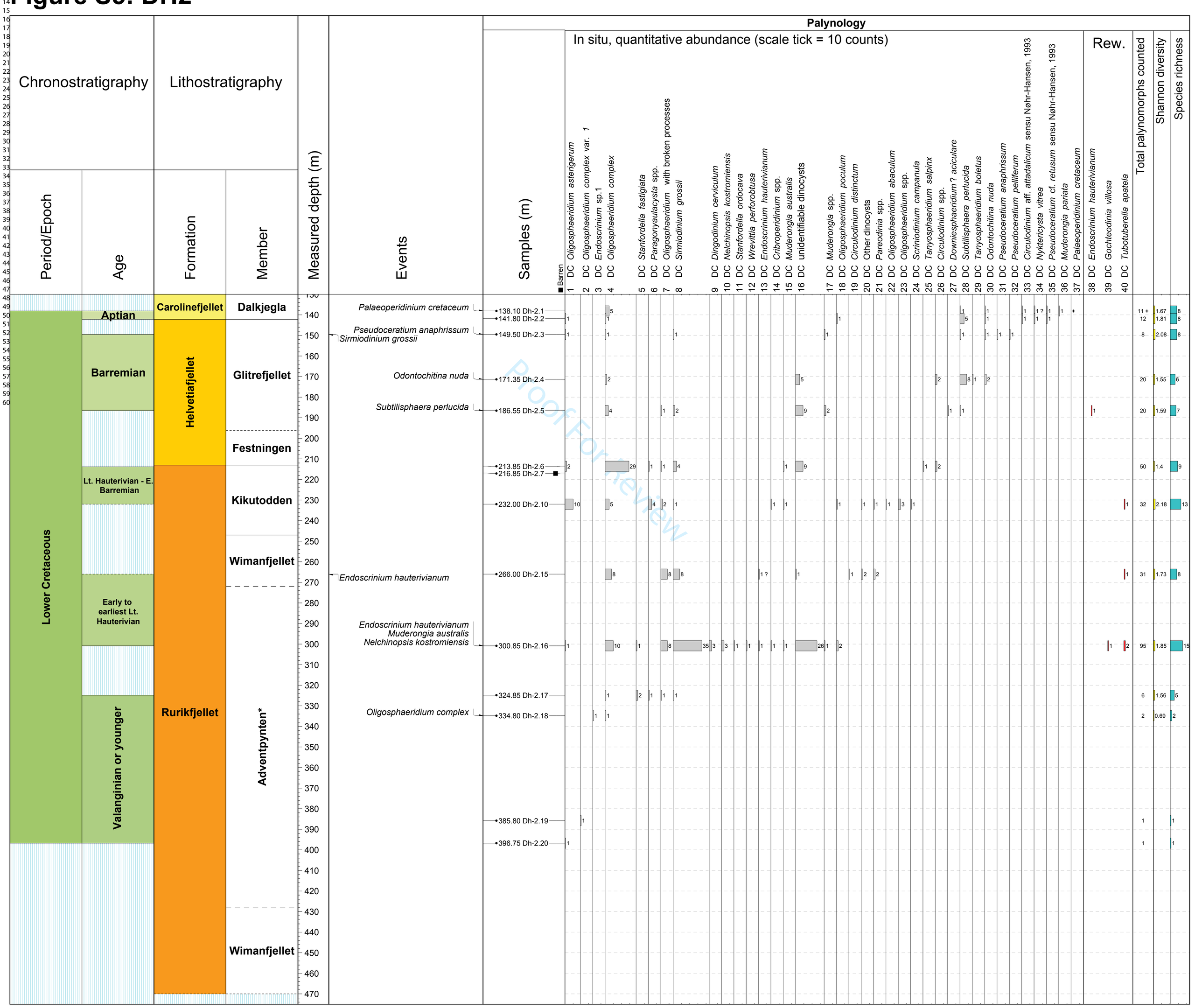

Figure S5. Distribution of dinocysts in the DH2 well.This file contains range charts with the quantitative data of the palynomorphs recognised in this study. The palynomorphs are arranged after the first occurrence (FO), R – reworked, DC – dinocyst, AC – acritarch, MP – palynomorph, “+” – present outside counting, “?” – questionable

Geological Magazine

Dinocyst stratigraphy of the Valanginian–Aptian Rurikfjellet and Helvetiafjellet formations on Spitsbergen, Arctic Norway

Kasia K. Śliwińska, Mads E. Jelby, Sten-Andreas Grundvåg, Henrik Nøhr-Hansen, Peter Alsen, and Snorre Olaussen

Supplementary material

Figure S6: DH5R

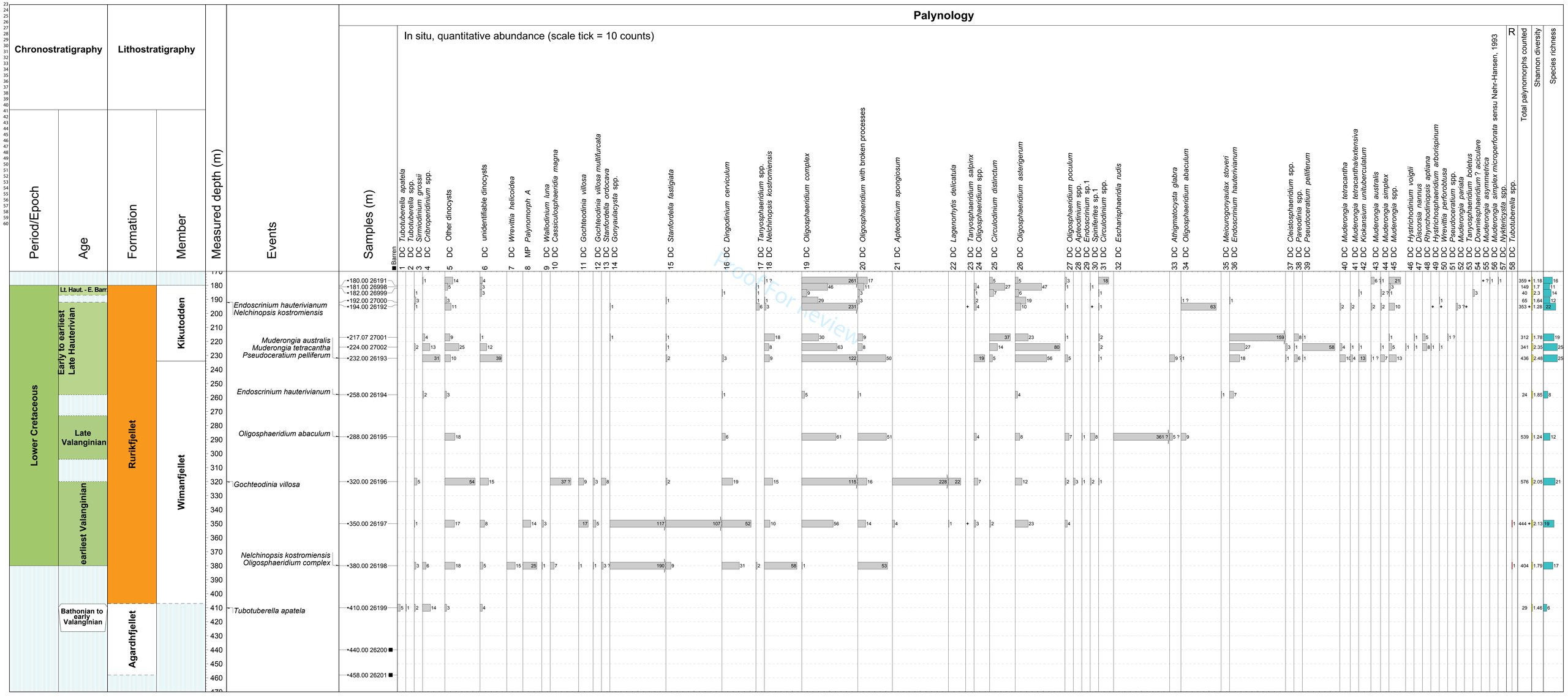

Figure S6. Distribution of dinocysts in the DH5R well. This file contains range charts with the quantitative data of the palynomorphs recognised in this study.
The palynomorphs are arranged after the first occurrence (FO), R – reworked, DC – dinocyst, AC – acritarch, MP – palynomorph, , "+" – present outside counting, "?" – questionable